Petroleum Science 19 (2022) 2720–2740

Contents lists available at ScienceDirect

Petroleum Science

journal homepage: www.keaipublishing.com/en/journals/petroleum-science

Original Paper

First-order approximate analytical expressions of oblique incident elastic wave at an interface of porous media saturated with a non-viscous fluid

Dong-Yong Zhou [a, b, *], Xing-Yao Yin [c], Xiao-Tao Wen [a, b], Xi-Lei He [a, b], Zhen-Hua He [a, b]

[a] State Key Laboratory of Oil and Gas Reservoir Geology and Exploitation, Chengdu University of Technology, Chengdu, Sichuan, 610059, China
[b] Key Laboratory of Earth Exploration and Information Technology of Ministry of Education, Chengdu University of Technology, Chengdu, Sichuan, 610059, China
[c] College of Geosciences and Technology, China University of Petroleum (East China), Qingdao, Shandong, 266580, China

ARTICLE INFO

Article history:
Received 17 January 2022
Received in revised form
29 June 2022
Accepted 16 October 2022
Available online 21 October 2022

Edited by Jie Hao

Keywords:
First-order approximate expressions
Oblique incident wave
Elastic plane wave
Porous media
Scattering coefficient

ABSTRACT

The analysis technology of Amplitude Variation with Offset (AVO) is one of the important methods for oil and gas reservoir prediction. Zoeppritz equation and its approximations are the theoretical basis of AVO analysis, which assumes that the upper and lower media of a horizontal interface are single-phase media. Limited by this assumption, AVO analysis has limited prediction and identification accuracy for complex porous reservoirs. In view of this, the first-order approximate analytical expressions of oblique elastic wave at an interface of porous media are derived. Firstly, the incident and scattering characteristics of various waves at the interface of porous media are analyzed, and the displacement vectors generated by these elastic waves are described by exponential function. Secondly, the kinematic and dynamic boundary conditions at the interface of porous media are discussed. Thirdly, by substituting the displacement vectors of incident and scattered waves into boundary conditions, the exact analytical equation is derived. Then, considering the symmetry of scattering matrix in the equation, the exact analytical expressions of each scattered wave are obtained. Furthermore, under the assumptions of small incident angle, weak elasticity at an interface of porous media, and ignoring the second- and higher-order terms, the first-order approximate analytical expressions are derived. Establishing a model of sandstone porous media with different porosity in upper and lower media, the correctness of the approximate analytical expressions is verified, and the elastic wave response characteristics of lithology and pore fluids are analyzed.

1. Introduction

Rock in seismic exploration can usually be considered as a two-phase body composed of rock skeleton and pore fluids. The rock properties are not only related to various mineral components that make up rock skeleton, but also affected by many factors, such as pore's size, shape, connectivity, and its filling. When an elastic wave propagates in such a media, it will produce complex reflection and transmission characteristics at the interface, which carry a lot of information related to rock skeleton, pores, and their fillings. Making full use of these information, the structural characteristics, rock properties, pores and pore fluid types of underground media can be identified to a certain extent, which makes it possible to predict oil and gas reservoir by using reflected elastic waves.

The variation of seismic wave amplitude with offset (AVO) includes elastic and physical properties of upper and lower media at formation interface. Zoeppritz equation lays the theoretical foundation for AVO analysis (Zoeppritz, 1919), which establishes the quantitative relationship between seismic data and incident angle, P-wave velocity, SV-wave velocity and density. However, the reflection and transmission information of the P- and SV-waves in the equation are coupled, which limits its application in the field of seismic exploration, although some research results have been obtained based on the equation in elastic parameter inversion (Lu et al., 2015; Gholami et al., 2018; Liu et al., 2021), oil and gas reservoir prediction (Huang et al., 2015; Pan et al., 2017; Passos et al., 2019; Sang et al., 2021), etc. As seismic exploration is

* Corresponding author. State Key Laboratory of Oil and Gas Reservoir Geology and Exploitation, Chengdu University of Technology, Chengdu, Sichuan, 610059, China.
E-mail address: zhou_dongyong@163.com (D.-Y. Zhou).

https://doi.org/10.1016/j.petsci.2022.10.009

mainly based on reflected wave (P- or SV-waves) information, it is necessary to decouple the reflected elastic waves from the equation and to derive exact or approximate expressions (Muskat and Meres, 1940; Bortfeld, 1962; Aki and Richards, 1980; Mallick, 1993; Wang, 1999; Santos and Tygel, 2004). The famous Aki and Richards approximation (Aki and Richards, 1980) lays the theoretical foundation for the prestack AVO inversion, which establishes an approximate linear relationship between the angle dependent reflection coefficient of the P- or SV-wave and the P-wave velocity, SV-wave velocity and density. Based on this approximation and combined with petrophysical theory, geophysicists have derived a series of deformation approximations (Shuey,1985; Smith and Gidlow,1987; Fatti et al., 1994; Gray et al., 1999), which are widely used in hydrocarbon reservoir prediction (Russell et al., 2003; Yin and Zhang, 2014; Zong et al., 2015, 2021; Chen et al., 2020).

Zoeppritz equation and its transformations assume that the upper and lower rocks at an interface are single-phase isotropic homogeneous media, which have limited applicable conditions for complex porous media saturated with pore fluids. With the development of elastic porous theory (Biot, 1941, 1957, 1962; Gassmann,1951; Smit,1961; Mojeddifar et al., 2015) and its application in oil and gas reservoir prediction (Chen et al., 2012; Chabyshova and Goloshubin, 2014; Yin et al., 2013, 2015; Sang et al., 2021), the scattering characteristics of elastic waves at the interface of porous media have attracted great attention of exploration geophysicists. The boundary conditions at an interface of porous media are much more complex than that of the single-phase media. In addition to considering the displacement and stress continuity of elastic solids at an interface, the effects of pore's size, structure and filling can also not be ignored (Deresiewicz and Skalak,1963; Deresiewicz,1974; Lovera,1987; Sharma and Gogna,1990; Sharma,2008). Following these studies, the reflection and transmission of elastic waves at an interface of porous media saturated with non-viscous fluids were considered, and the seismic wave response characteristics of pores and pore fluids were analyzed (Vashisth et al., 1991; Denneman et al., 2002; Kumar et al., 2011; Liu and Greenhalgh, 2014; Zhou et al., 2019).

The viscosity of pore fluids in complex porous media can not be ignored. This property causes dispersion and attenuation of elastic waves propagating in porous media, resulting in the change of reflection and transmission characteristics (Yang and Sato,1998; Kumar et al., 2013; Kumari,2014; Kumari et al., 2017, 2021). For more complex porous media, such as carbonate reservoir, reef and beach reservoir, etc., the pore contains two or more fluids. The type of pore fluids, volume ratio among pore fluids, and interaction between pore fluids and rock skeleton will affect the scattering characteristics of elastic waves at the interface (Drew et al., 1979; Tomar and Arora, 2006; Arora and Tomar,2007; Lo et al., 2009; Yeh et al., 2010; Dai et al., 2006). Their researches analyze the variation of elastic wave amplitude with offset for different types of porous media, that is, Zoeppritz equation of different two-phase media. While the reflection and transmission information of the fast P-, SV-, and slow P-waves are coupled, which makes it difficult to independently analyze the relative influence of lithologic and pore fluid parameters on the scattering coefficients of elastic waves. The exact and approximate analytical methods are relatively simple and practical expressions, which are also more convenient for the analysis of elastic wave response characteristics of various lithology and pore fluid parameters (Gurevich et al., 2004; Kumar et al., 2018, 2019; Yuan et al., 2020). At present, the approximate expressions of scattering coefficients of an elastic wave perpendicular at an interface of porous media had been derived (Gurevich et al., 2004; Silin et al., 2004; Silin and Goloshubin, 2010; Zhou et al., 2020; Carcione et al., 2021).

The approximate expressions of scattering coefficient of an elastic wave incident at an interface of porous media at any angle have not been studied. Compared with vertically reflected elastic wave, prestack seismic data contains more abundant amplitude information. Based on previous researches, considering boundary conditions at the interface of porous media saturated with a non-viscous fluid, an exact equation of scattering coefficient is firstly derived. Further simplifying the equation, and fully considering the symmetry of its scattering matrix, the exact analytical expressions of various scattering coefficients can be obtained. Under various priori assumptions, the first-order approximate analytical expressions of scattering coefficients are finally derived.

2. Analytical equation

2.1. Displacement and stress-strain

The displacement vectors of porous media caused by the propagation of the fast P-, SV-, and slow P-waves, $\mathbf{U}^P$, $\mathbf{U}^{SV}$, $\mathbf{U}^B$, and the total displacement vector of porous media, $\mathbf{U}_{\text{total}}$, can be expressed as,

$$\mathbf{U}^P = \begin{bmatrix} U_x^P & U_y^P & U_z^P \end{bmatrix} = \begin{bmatrix} \frac{\partial \phi}{\partial x} & 0 & \frac{\partial \phi}{\partial z} \end{bmatrix} \tag{1}$$

$$\mathbf{U}^{SV} = \begin{bmatrix} U_x^{SV} & U_y^{SV} & U_z^{SV} \end{bmatrix} = \begin{bmatrix} -\frac{\partial \psi}{\partial z} & 0 & \frac{\partial \psi}{\partial x} \end{bmatrix} \tag{2}$$

$$\mathbf{U}^B = \begin{bmatrix} U_x^B & U_y^B & U_z^B \end{bmatrix} = \begin{bmatrix} \frac{\partial \varphi}{\partial x} & 0 & \frac{\partial \varphi}{\partial z} \end{bmatrix} \tag{3}$$

$$\mathbf{U}_{\text{total}} = \mathbf{U}^P + \mathbf{U}^{SV} + \mathbf{U}^B = \begin{bmatrix} U_x & U_y & U_z \end{bmatrix} \tag{4}$$

Here, the symbols of ϕ, ψ, φ represent the wave functions of the fast P-, SV-, and slow P-waves, and the operators of $\frac{\partial}{\partial x}$, $\frac{\partial}{\partial z}$ denote the partial derivatives of x, z, respectively. The superscripts of P, SV, B represent the fast P-, SV-, and slow P-waves, and the subscripts of x, y, z denote along the directions of x, y, z, respectively. For example, the symbol of U_x^P represents the displacement component of porous media along the direction of x caused by the fast P-wave.

Following Silin and Goloshubin (2010), the stresses between rock skeletons caused by the fluctuations of the fast P- and SV-waves, $\boldsymbol{\tau}^P$ and $\boldsymbol{\tau}^{SV}$, and the total stress between rock skeletons, $\boldsymbol{\tau}_{\text{skeleton}}$, can be expressed as,

$$\boldsymbol{\tau}^P = \begin{bmatrix} \tau_x^P & \tau_y^P & \tau_z^P \end{bmatrix} = \begin{bmatrix} 2\mu \frac{\partial^2 \phi}{\partial z \partial x} & 0 & \left(K - \frac{2}{3}\mu\right)\nabla^2 \phi + 2\mu \frac{\partial^2 \phi}{\partial z^2} \end{bmatrix} \tag{5}$$

$$\boldsymbol{\tau}^{SV} = \begin{bmatrix} \tau_x^{SV} & \tau_y^{SV} & \tau_z^{SV} \end{bmatrix} = \begin{bmatrix} \mu\left(\frac{\partial^2 \psi}{\partial x^2} - \frac{\partial^2 \psi}{\partial z^2}\right) & 0 & 2\mu \frac{\partial^2 \psi}{\partial z \partial x} \end{bmatrix} \tag{6}$$

$$\boldsymbol{\tau}_{\text{skeleton}} = \boldsymbol{\tau}^P + \boldsymbol{\tau}^{SV} = K(\nabla \cdot \mathbf{U}_{\text{total}})\mathbf{I} + \mu\left[\nabla \mathbf{U}_{\text{total}} + (\nabla \mathbf{U}_{\text{total}})^T - \frac{2}{3}(\nabla \cdot \mathbf{U}_{\text{total}})\mathbf{I}\right] \tag{7}$$

Here, the symbols of K, μ represent the bulk and shear moduli of rock skeleton, respectively, and the superscript T denotes transposition. The operators of $\frac{\partial^2}{\partial x^2}$, $\frac{\partial^2}{\partial z^2}$, ∇, $\nabla\cdot$, and ∇^2 represent quadratic partial derivative for x, quadratic partial derivative for z, Gradient operator, Divergence operator, and Laplace operator, respectively. For example, τ_x^P denotes the shear stress along the direction of x between rock skeletons caused by the fast P-wave.

The displacement vector of pore fluid relative to rock skeleton, $\mathbf{W}$, the static pressure of pore fluids, $\mathbf{P}$, and the total stress between two pore media, $\boldsymbol{\tau}_{\text{total}}$, can be expressed as,

$$\mathbf{W} = \delta^{P}\mathbf{U}^{P} + \delta^{SV}\mathbf{U}^{SV} + \delta^{B}\mathbf{U}^{B} \tag{8}$$

$$\mathbf{P} = [-\overline{\alpha}\overline{M}\nabla\cdot\mathbf{U}_{\text{total}} - \overline{M}\nabla\cdot\mathbf{W}]\cdot\mathbf{I} \tag{9}$$

$$\tau_{\text{total}} = \tau_{\text{skeleton}} - \overline{\alpha}\cdot\mathbf{P} \tag{10}$$

where, the symbols of $\overline{\alpha}$ and $\overline{M}$ represent Biot's parameters, and $\mathbf{I}$ is identity matrix. The symbols of $\delta^{P}, \delta^{SV}, \delta^{B}$ denote the ratios between the displacement amplitude of pore fluid relative to rock skeleton and that of rock skeleton caused by the fast P-, SV-, and slow P-waves, respectively.

2.2. Scattering matrix

Different from single-phase media, describing porous media requires more lithology and fluid parameters, mainly including: rock physical parameters (porosity φ', rock matrix density ρ^{s}), rock skeleton parameters (bulk modulus K^{d} and shear modulus μ^{d} of rock skeleton), Biot's parameters ($\overline{\alpha}$ and$\overline{M}$), and pore fluid parameters (bulk modulus K^{d}, viscosity coefficient η^{f}, and fluid density ρ^{f}). When a plane wave is reflected or transmitted at an interface between two porous media, it also includes velocity parameters (fast P-wave α, SV-wave β, and slow P-wave γ), and incident, reflected, and transmitted angles (fast P-wave i, SV-wave j, and slow P-wave k), as shown in Fig. 1.

In Fig. 1, the upper and lower media of a horizontal interface are isotropic porous media saturated with pore fluids, and two media are assumed in seamless contact. In the upper porous medium, there are three kinds of elastic waves incident at the horizontal interface (fast P-wave $\searrow P_1$, SV-wave $\searrow S_1$, and slow P-wave $\searrow B_1$), and there are also three kinds of elastic waves reflected from the interface to the upper porous medium (fast P-wave $\nearrow P_1$, SV-wave $\nearrow S_1$, and slow P-wave $\nearrow B_1$). Similarly, there are three kinds of incident waves (fast P-wave $\nearrow P_2$, SV-wave $\nearrow S_2$, and slow P-wave $\nearrow B_2$), and three kinds of reflected waves (fast P-wave $\searrow P_2$, SV-wave $\searrow S_2$, and slow P-wave $\searrow B_2$) in the lower porous medium. The displacement vectors of the six incident waves can be described by the expressions in Table 1. We use the superscripts of ↗ and ↘ to represent the up and down traveling waves, respectively, and the subscripts of 1 and 2 to represent the upper and lower media, respectively.

Each incident wave will produce three reflected waves and three transmitted waves at the horizontal interface, as shown in Fig. 2. Fig. 2(a), (c), and 2(e) show the reflection and transmission with incident waves of the upper medium being the fast P-, SV-, and slow P-waves, respectively, and the corresponding displacement vectors of the reflected and transmitted waves are shown in Tables 2(a), 2(c), and 2(e), respectively. Fig. 2(b), (d), and 2(f) represent the reflection and transmission with incident waves of the lower medium being the fast P-, SV-, and slow P-waves, respectively, and the corresponding displacement vectors of the reflected and transmitted waves are shown in Tables 2(b), 2(d), and 2(f), respectively. For example, the symbol of $\searrow\nearrow PS$ represents the reflection coefficient with incident fast P-wave and reflected SV-wave.

Similar to Aki and Richards (1980), 36 kinds of reflection and transmission coefficients at the interface between two porous media can form a **Scattering Matrix** as shown in Eq. (11), which can be calculated by the continuity of stress and displacement of rock skeleton (and pore fluids) along the x and z directions.

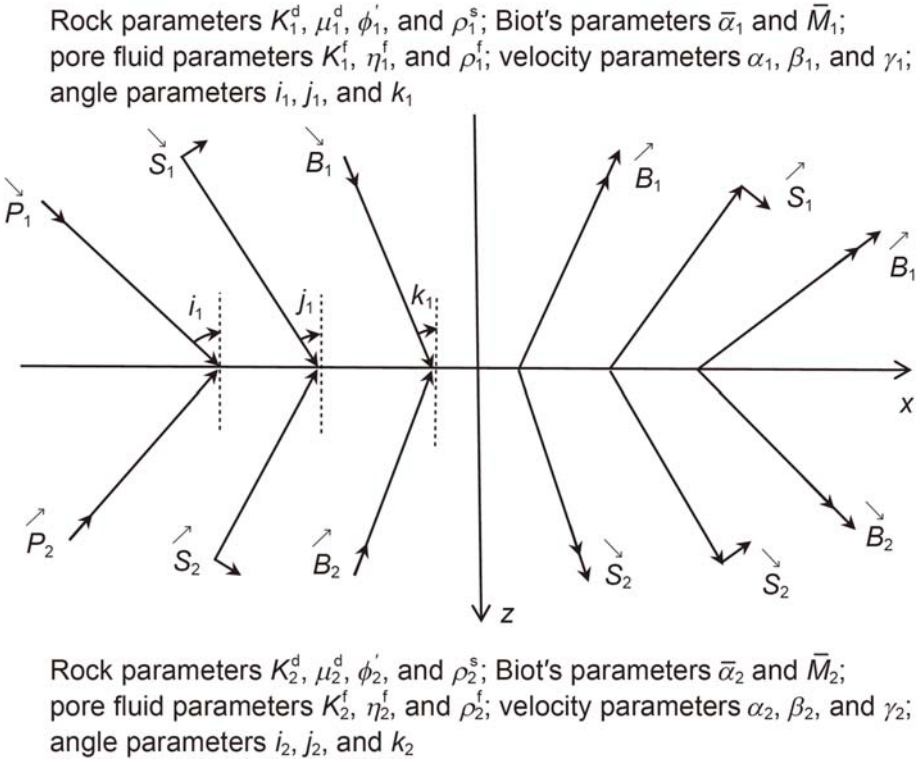

Fig. 1. Complete system of incident and scattering for P-SV-B plane waves.
The short arrows indicate the direction of wave's vibration, and the long arrows denote the propagation direction.

Table 1
Displacement vectors of P-SV-B incident waves.

Medium	Type	Displacement
Upper medium	Downgoing *P*	$S(\sin i_1 \quad 0 \quad \cos i_1)\exp\left[i\omega\left(px+\frac{\cos i_1}{\alpha_1}z-t\right)\right]$
	Downgoing *SV*	$S(\cos j_1 \quad 0 \quad -\sin j_1)\exp\left[i\omega\left(px+\frac{\cos j_1}{\beta_1}z-t\right)\right]$
	Downgoing *B*	$S(\sin k_1 \quad 0 \quad \cos k_1)\exp\left[i\omega\left(px+\frac{\cos k_1}{\gamma_1}z-t\right)\right]$
Lower medium	Upgoing *P*	$S(\sin i_2 \quad 0 \quad -\cos i_2)\exp\left[i\omega\left(px-\frac{\cos i_2}{\alpha_2}z-t\right)\right]$
	Upgoing *SV*	$S(\cos j_2 \quad 0 \quad \sin j_2)\exp\left[i\omega\left(px-\frac{\cos j_2}{\beta_2}z-t\right)\right]$
	Upgoing *B*	$S(\sin k_2 \quad 0 \quad -\cos k_2)\exp\left[i\omega\left(px-\frac{\cos k_2}{\gamma_2}z-t\right)\right]$

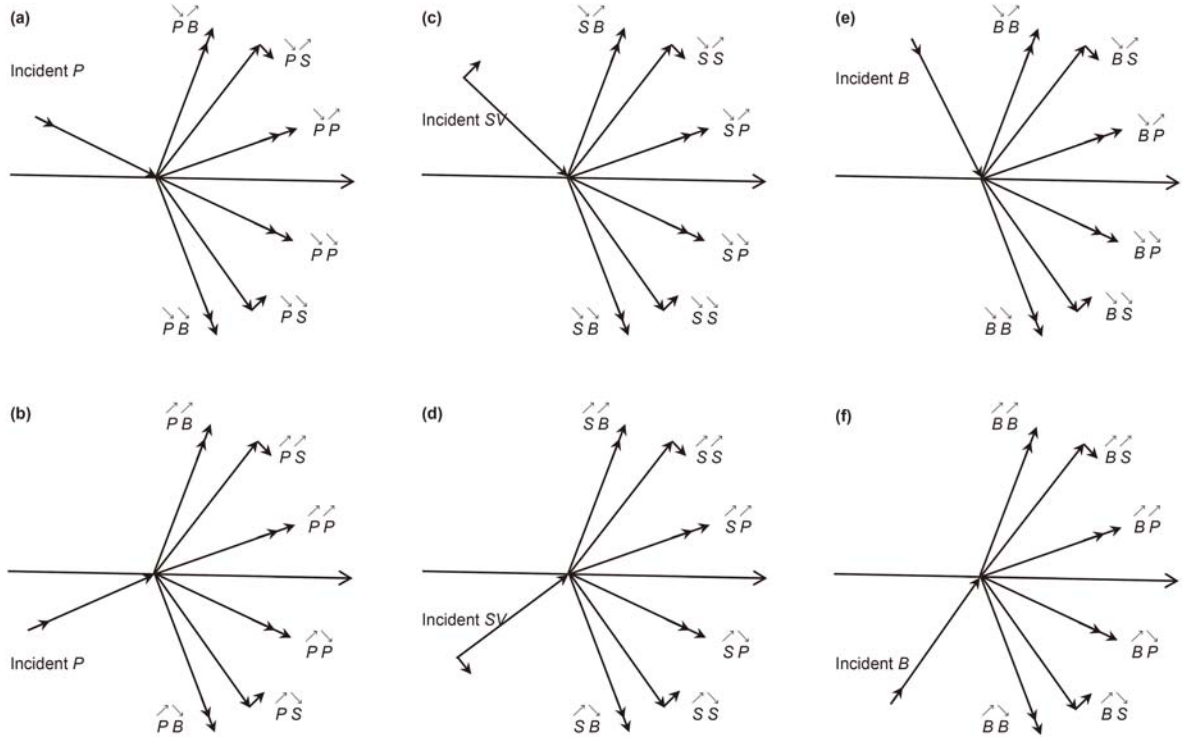

Fig. 2. 36 kinds of reflection and transmission coefficients generated by P-SV-B plane wave system. The short arrows indicate the direction of wave's vibration, and the long arrows denote the propagation direction.

$$R\&T = \begin{bmatrix} \overleftarrow{P}\overrightarrow{P} & \overleftarrow{P}\overleftarrow{P} & \overleftarrow{S}\overrightarrow{P} & \overleftarrow{S}\overleftarrow{P} & \overleftarrow{B}\overrightarrow{P} & \overleftarrow{B}\overleftarrow{P} \\ \overleftarrow{P}\overrightarrow{S} & \overleftarrow{P}\overleftarrow{S} & \overleftarrow{S}\overrightarrow{S} & \overleftarrow{S}\overleftarrow{S} & \overleftarrow{B}\overrightarrow{S} & \overleftarrow{B}\overleftarrow{S} \\ \overleftarrow{P}\overrightarrow{B} & \overleftarrow{P}\overleftarrow{B} & \overleftarrow{S}\overrightarrow{B} & \overleftarrow{S}\overleftarrow{B} & \overleftarrow{B}\overrightarrow{B} & \overleftarrow{B}\overleftarrow{B} \\ \overrightarrow{P}\overrightarrow{P} & \overrightarrow{P}\overleftarrow{P} & \overrightarrow{S}\overrightarrow{P} & \overrightarrow{S}\overleftarrow{P} & \overrightarrow{B}\overrightarrow{P} & \overrightarrow{B}\overleftarrow{P} \\ \overrightarrow{P}\overrightarrow{S} & \overrightarrow{P}\overleftarrow{S} & \overrightarrow{S}\overrightarrow{S} & \overrightarrow{S}\overleftarrow{S} & \overrightarrow{B}\overrightarrow{S} & \overrightarrow{B}\overleftarrow{S} \\ \overrightarrow{P}\overrightarrow{B} & \overrightarrow{P}\overleftarrow{B} & \overrightarrow{S}\overrightarrow{B} & \overrightarrow{S}\overleftarrow{B} & \overrightarrow{B}\overrightarrow{B} & \overrightarrow{B}\overleftarrow{B} \end{bmatrix} \tag{11}$$

2.3. Approximate analytical equation

The boundary conditions at an interface of porous media saturated with pore fluids are determined by their existing physical conditions. Generally, the energy conservation and fluidity fluid continuity equation at the interface are used as a basic ideas for analyzing boundary conditions (Sharma, 2008). Following Silin and Goloshubin (2010) and Zhou et al. (2019), the boundary conditions at an interface of porous media include kinematics [tangential displacement of rock skeleton U_x, vertical displacement of rock skeleton U_z, and displacement of pore fluids W_z] and dynamics [total tangential stress $(\tau_{\text{total}})_x$, total vertical stress $(\tau_{\text{total}})_z$, and pore fluid static pressure P_z].

Displacement vectors (Eqs. (1)~(4) and (8)) and stress vectors (Eqs. (5)~(7) and (9)) are substituted into the boundary conditions (Eq. (12)), and assuming that the velocities and corresponding incident angles of three elastic waves meet Snell's law (Eq. (13)), the expressions of incident, reflected and transmitted amplitudes described by incident and reflection angles, elastic and physical parameters, Biot's parameters, displacement potential amplitude ratio, and other parameters can be derived (Eq. (14)).

$$\begin{bmatrix} U_x \\ U_z \\ W_z \\ (\tau_{\text{total}})_x \\ (\tau_{\text{total}})_z \\ P_z \end{bmatrix}_1 = \begin{bmatrix} U_x \\ U_z \\ W_z \\ (\tau_{\text{total}})_x \\ (\tau_{\text{total}})_z \\ P_z \end{bmatrix}_2 \tag{12}$$

By writing Eq. (14) into the forms of matrix and vector, the exact analytical equation of oblique incident wave can be obtained as Eq. (15). Following the ideas of Aki and Richards (1980) and Chaisri and Krebes (2000), the scattering matrix in Eq. (11) can be obtained by solving Eq. (16) and making elementary changes.

The parameters and combinations in the coefficient matrix of Eq. (15) can be further approximated and simplified (See Appendix A). Eqs. A-1~A-6 is substituted into Eq. (15), then the approximate analytical equation can be simplified as Eq. (17). By analyzing Eqs. (17a) and (17b), we can see that the scattering coefficient to be solved in Eq. (16) can be expressed by 9 submatrices of $\langle \mathbf{1} \rangle \sim \langle \mathbf{9} \rangle$, which need to be obtained by solving matrix $\mathbf{L}^{-1}\mathbf{N}$. For solving it, we need to fully consider the similarity of parameters in matrices $\mathbf{L}$ and $\mathbf{N}$, that is, they can be described by 9 two-dimensional submatrices $\mathbf{A} \sim \mathbf{K}$, which provides convenience for the solution of Eq. (17c).

$$p = \frac{\sin i_1}{\alpha_1} = \frac{\sin j_1}{\beta_1} = \frac{\sin k_1}{\gamma_1} = \frac{\sin i_2}{\alpha_2} = \frac{\sin j_2}{\beta_2} = \frac{\sin k_2}{\gamma_2} \tag{13}$$

$$\begin{aligned} &\sin i_1\left(\breve{P}_1 + \acute{P}_1\right) + \cos j_1\left(\breve{S}_1 + \acute{S}_1\right) + \sin k_1\left(\breve{B}_1 + \acute{B}_1\right) = \\ &\sin i_2\left(\breve{P}_2 + \acute{P}_2\right) + \cos j_2\left(\searrow S_2 + \nearrow S_2\right) + \sin k_2\left(\searrow B_2 + \nearrow B_2\right) \end{aligned} \tag{14a}$$

$$\begin{aligned} &\cos i_1\left(\breve{P}_1 - \acute{P}_1\right) - \sin j_1\left(\breve{S}_1 - \acute{S}_1\right) + \cos k_1\left(\breve{B}_1 - \acute{B}_1\right) = \\ &\cos i_2\left(\breve{P}_2 - \acute{P}_2\right) - \sin j_2\left(\breve{S}_2 - \acute{S}_2\right) + \cos k_2\left(\breve{B}_2 - \acute{B}_2\right) \end{aligned} \tag{14b}$$

$$\begin{aligned} &\delta_1^P \cos i_1\left(\breve{P}_1 - \acute{P}_1\right) - \delta_1^{SV} \sin j_1\left(\breve{S}_1 - \acute{S}_1\right) + \delta_1^B \cos k_1\left(\breve{B}_1 - \acute{B}_1\right) = \\ &\delta_2^P \cos i_2\left(\breve{P}_2 - \acute{P}_2\right) - \delta_2^{SV} \sin j_2\left(\breve{S}_2 - \acute{S}_2\right) + \delta_2^B \cos k_2\left(\breve{B}_2 - \acute{B}_2\right) \end{aligned} \tag{14c}$$

$$\begin{aligned} &2p\mu_1 \cos i_1\left(\breve{P}_1 - \acute{P}_1\right) + \frac{\mu_1}{\beta_1}\left(1 - 2\beta_1^2 p^2\right)\left(\breve{S}_1 - \acute{S}_1\right) + 2p\mu_1 \cos k_1\left(\breve{B}_1 - \acute{B}_1\right) = \\ &2p\mu_2 \cos i_2\left(\breve{P}_2 - \acute{P}_2\right) + \frac{\mu_2}{\beta_2}\left(1 - 2\beta_2^2 p^2\right)\left(\breve{S}_2 - \acute{S}_2\right) + 2p\mu_2 \cos k_2\left(\breve{B}_2 - \acute{B}_2\right) \end{aligned} \tag{14d}$$

$$\begin{aligned} &\frac{1}{\alpha_1}\left[\left(K_1 + \overline{\alpha}_1^2\overline{M}_1 - \frac{2}{3}\mu_1 + \delta_1^P\overline{\alpha}_1\overline{M}_1\right) + 2\mu_1\left(1 - \alpha_1^2 p^2\right)\right] \\ &\times \left(\breve{P}_1 + \acute{P}_1\right) - 2\mu_1 p\sqrt{1 - \beta_1^2 p^2}\left(\breve{S}_1 + \acute{S}_1\right) + \frac{1}{\gamma_1}\Big[\\ &\times \left(K_1 + \overline{\alpha}_1^2\overline{M}_1 - \frac{2}{3}\mu_1 + \delta_1^B\overline{\alpha}_1\overline{M}_1\right) + 2\mu_1\left(1 - \gamma_1^2 p^2\right)\Big]\left(\breve{B}_1 + \acute{B}_1\right) = \frac{1}{\alpha_2}\Big[\\ &\times \left(K_2 + \overline{\alpha}_2^2\overline{M}_2 - \frac{2}{3}\mu_2 + \delta_2^P\overline{\alpha}_2\overline{M}_2\right) + 2\mu_2\left(1 - \alpha_2^2 p^2\right)\Big] \\ &\times \left(\breve{P}_2 + \acute{P}_2\right) - 2\mu_2 p\sqrt{1 - \beta_2^2 p^2}\left(\breve{S}_2 + \acute{S}_2\right) + \frac{1}{\gamma_2}\Big[\\ &\times \left(K_2 + \overline{\alpha}_2^2\overline{M}_2 - \frac{2}{3}\mu_2 + \delta_2^B\overline{\alpha}_2\overline{M}_2\right) + 2\mu_2\left(1 - \gamma_2^2 p^2\right)\Big]\left(\breve{B}_2 + \acute{B}_2\right) \end{aligned} \tag{14e}$$

$$\begin{aligned} &-\frac{\left(\overline{\alpha}_1 + \delta_1^P\right)\overline{M}_1}{\alpha_1}\left(\breve{P}_1 + \acute{P}_1\right) - 0\cdot\left(\breve{S}_1 + \acute{S}_1\right) - \frac{\left(\overline{\alpha}_1 + \delta_1^B\right)\overline{M}_1}{\gamma_1}\left(\breve{B}_1 + \acute{B}_1\right) \\ &= -\frac{\left(\overline{\alpha}_2 + \delta_2^P\right)\overline{M}_2}{\alpha_2}\left(\breve{P}_2 + \acute{P}_2\right) - 0\cdot\left(\breve{S}_2 + \acute{S}_2\right) - \frac{\left(\overline{\alpha}_2 + \delta_2^B\right)\overline{M}_2}{\gamma_2}\left(\breve{B}_2 + \acute{B}_2\right) \end{aligned} \tag{14f}$$

$$\begin{bmatrix} -\sin i_1 & \sin i_2 & -\sin k_1 & \sin k_2 \\ \frac{1}{\alpha_1}\left[\left(K_1 + \overline{\alpha}_1^2\overline{M}_1 - \frac{2}{3}\mu_1 + \delta_1^P\overline{\alpha}_1\overline{M}_1\right) + 2\mu_1\left(1 - \alpha_1^2 p^2\right)\right] & -\frac{1}{\alpha_2}\left[\left(K_2 + \overline{\alpha}_2^2\overline{M}_2 - \frac{2}{3}\mu_2 + \delta_2^P\overline{\alpha}_2\overline{M}_2\right) + 2\mu_2\left(1 - \alpha_2^2 p^2\right)\right] & \frac{1}{\gamma_1}\left[\left(K_1 + \overline{\alpha}_1^2\overline{M}_1 - \frac{2}{3}\mu_1 + \delta_1^B\overline{\alpha}_1\overline{M}_1\right) + 2\mu_1\left(1 - \gamma_1^2 p^2\right)\right] & -\frac{1}{\gamma_2}\left[\left(K_2 + \overline{\alpha}_2^2\overline{M}_2 - \frac{2}{3}\mu_2 + \delta_2^B\overline{\alpha}_2\overline{M}_2\right) + 2\mu_2\left(1 - \gamma_2^2 p^2\right)\right] \\ \cos i_1 & \cos i_2 & \cos k_1 & \cos k_2 \\ 2p\mu_1 \cos i_1 & 2p\mu_2 \cos i_2 & 2p\mu_1 \cos k_1 & 2p\mu_2 \cos k_2 \\ \delta_1^P \cos i_1 & \delta_2^P \cos i_2 & \delta_1^B \cos k_1 & \delta_2^B \cos k_2 \\ -\frac{\left(\overline{\alpha}_1 + \delta_1^P\right)\overline{M}_1}{\alpha_1} & \frac{\left(\overline{\alpha}_2 + \delta_2^P\right)\overline{M}_2}{\alpha_2} & -\frac{\left(\overline{\alpha}_1 + \delta_1^B\right)\overline{M}_1}{\gamma_1} & \frac{\left(\overline{\alpha}_2 + \delta_2^B\right)\overline{M}_2}{\gamma_2} \\ -\cos j_1 & \cos j_2 & \sin k_1 & -\sin k_2 \\ 2p\mu_1 \cos j_1 & -2p\mu_2 \cos j_2 & -2p\mu_1 \cos k_1 & 2p\mu_2 \cos k_2 \\ -\sin j_1 & \frac{\mu_2}{\beta_2}\left(1 - 2\beta_2^2 p^2\right) & \frac{\mu_1}{\beta_1}\left(1 - 2\beta_1^2 p^2\right) & -\frac{\mu_2}{\beta_2}\left(1 - 2\beta_2^2 p^2\right) \\ -\delta_1^{SV} \sin j_1 & -\delta_2^{SV} \sin j_2 & \delta_1^{SV} \sin j_1 & -\delta_2^{SV} \sin j_2 \\ 0 & 0 & 0 & 0 \end{bmatrix} \cdot \begin{bmatrix} \nwarrow P_1 \\ \nearrow P_2 \\ \nwarrow S_1 \\ \nearrow S_2 \\ \nwarrow B_1 \\ \nearrow B_2 \end{bmatrix} = \begin{bmatrix} \sin i_1 & -\sin i_2 & \sin k_1 & -\sin k_2 \\ \frac{1}{\alpha_1}\left[\left(K_1 + \overline{\alpha}_1^2\overline{M}_1 - \frac{2}{3}\mu_1 + \delta_1^P\overline{\alpha}_1\overline{M}_1\right) + 2\mu_1\left(1 - \alpha_1^2 p^2\right)\right] & -\frac{1}{\alpha_2}\left[\left(K_2 + \overline{\alpha}_2^2\overline{M}_2 - \frac{2}{3}\mu_2 + \delta_2^P\overline{\alpha}_2\overline{M}_2\right) + 2\mu_2\left(1 - \alpha_2^2 p^2\right)\right] & \frac{1}{\gamma_1}\left[\left(K_1 + \overline{\alpha}_1^2\overline{M}_1 - \frac{2}{3}\mu_1 + \delta_1^B\overline{\alpha}_1\overline{M}_1\right) + 2\mu_1\left(1 - \gamma_1^2 p^2\right)\right] & -\frac{1}{\gamma_2}\left[\left(K_2 + \overline{\alpha}_2^2\overline{M}_2 - \frac{2}{3}\mu_2 + \delta_2^B\overline{\alpha}_2\overline{M}_2\right) + 2\mu_2\left(1 - \gamma_2^2 p^2\right)\right] \\ \cos i_1 & \cos i_2 & \cos k_1 & \cos k_2 \\ 2p\mu_1 \cos i_1 & 2p\mu_2 \cos i_2 & 2p\mu_1 \cos k_1 & 2p\mu_2 \cos k_2 \\ \delta_1^P \cos i_1 & \delta_2^P \cos i_2 & \delta_1^B \cos k_1 & \delta_2^B \cos k_2 \\ -\frac{\left(\overline{\alpha}_1 + \delta_1^P\right)\overline{M}_1}{\alpha_1} & \frac{\left(\overline{\alpha}_2 + \delta_2^P\right)\overline{M}_2}{\alpha_2} & -\frac{\left(\overline{\alpha}_1 + \delta_1^B\right)\overline{M}_1}{\gamma_1} & \frac{\left(\overline{\alpha}_2 + \delta_2^B\right)\overline{M}_2}{\gamma_2} \\ \sin j_1 & -\cos j_2 & -\cos j_1 & \cos j_2 \\ -2p\mu_1 \cos j_1 & 2p\mu_2 \cos j_2 & 2p\mu_1 \cos j_1 & -2p\mu_2 \cos j_2 \\ -\sin j_1 & \frac{\mu_2}{\beta_2}\left(1 - 2\beta_2^2 p^2\right) & \frac{\mu_1}{\beta_1}\left(1 - 2\beta_1^2 p^2\right) & -\frac{\mu_2}{\beta_2}\left(1 - 2\beta_2^2 p^2\right) \\ -\delta_1^{SV} \sin j_1 & -\delta_2^{SV} \sin j_2 & \delta_1^{SV} \sin j_1 & -\delta_2^{SV} \sin j_2 \\ 0 & 0 & 0 & 0 \end{bmatrix} \cdot \begin{bmatrix} \nearrow P_1 \\ \nwarrow P_2 \\ \searrow S_1 \\ \nwarrow S_2 \\ \nearrow B_1 \\ \nwarrow B_2 \end{bmatrix} \tag{15}$$

$$\mathbf{L}\cdot\begin{bmatrix}\overleftarrow{P}_1\\ \overrightarrow{P}_2\\ \overleftarrow{S}_1\\ \overrightarrow{S}_2\\ \overleftarrow{B}_1\\ \overrightarrow{B}_2\end{bmatrix}=\mathbf{N}\cdot\begin{bmatrix}\overrightarrow{P}_1\\ \overleftarrow{P}_2\\ \overrightarrow{S}_1\\ \overleftarrow{S}_2\\ \overrightarrow{B}_1\\ \overleftarrow{B}_2\end{bmatrix}\Rightarrow\mathbf{L}^{-1}\mathbf{N}=\begin{bmatrix}\overrightarrow{P}\overleftarrow{P} & \overleftarrow{P}\overleftarrow{P} & \overrightarrow{S}\overleftarrow{P} & \overleftarrow{S}\overleftarrow{P} & \overrightarrow{B}\overleftarrow{P} & \overleftarrow{B}\overleftarrow{P}\\ \overrightarrow{P}\overrightarrow{P} & \overleftarrow{P}\overrightarrow{P} & \overrightarrow{S}\overrightarrow{P} & \overleftarrow{S}\overrightarrow{P} & \overrightarrow{B}\overrightarrow{P} & \overleftarrow{B}\overrightarrow{P}\\ \overrightarrow{P}\overleftarrow{S} & \overleftarrow{P}\overleftarrow{S} & \overrightarrow{S}\overleftarrow{S} & \overleftarrow{S}\overleftarrow{S} & \overrightarrow{B}\overleftarrow{S} & \overleftarrow{B}\overleftarrow{S}\\ \overrightarrow{P}\overrightarrow{S} & \overleftarrow{P}\overrightarrow{S} & \overrightarrow{S}\overrightarrow{S} & \overleftarrow{S}\overrightarrow{S} & \overrightarrow{B}\overrightarrow{S} & \overleftarrow{B}\overrightarrow{S}\\ \overrightarrow{P}\overleftarrow{B} & \overleftarrow{P}\overleftarrow{B} & \overrightarrow{S}\overleftarrow{B} & \overleftarrow{S}\overleftarrow{B} & \overrightarrow{B}\overleftarrow{B} & \overleftarrow{B}\overleftarrow{B}\\ \overrightarrow{P}\overrightarrow{B} & \overleftarrow{P}\overrightarrow{B} & \overrightarrow{S}\overrightarrow{B} & \overleftarrow{S}\overrightarrow{B} & \overrightarrow{B}\overrightarrow{B} & \overleftarrow{B}\overrightarrow{B}\end{bmatrix}\tag{16}$$

$$\mathbf{L}\approx\begin{bmatrix}-\alpha_1 p & \alpha_2 p & -\cos j_1 & \cos j_2 & -\gamma_1 p & \gamma_2 p\\ -\rho_1\alpha_1\left(1-2\beta_1^2p^2\right) & \rho_2\alpha_2\left(1-2\beta_2^2p^2\right) & 2\rho_1\beta_1^2 p\cos j_1 & -2\rho_2\beta_2^2 p\cos j_2 & -\rho_1\gamma_1\left(1-2\beta_1^2p^2\right) & \rho_2\gamma_2\left(1-2\beta_2^2p^2\right)\\ \cos i_1 & \cos i_2 & -\beta_1 p & -\beta_2 p & 1 & 1\\ 2\rho_1\beta_1^2 p\cos i_1 & 2\rho_2\beta_2^2 p\cos i_2 & \rho_1\beta_1\left(1-2\beta_1^2p^2\right) & \rho_2\beta_2\left(1-2\beta_2^2p^2\right) & 2\rho_1\beta_1^2 p & 2\rho_2\beta_2^2 p\\ 0 & 0 & & & \delta_1^B & \delta_2^B\\ \dfrac{\overline{\alpha}_1\overline{M}_1}{\alpha_1} & -\dfrac{\overline{\alpha}_2\overline{M}_2}{\alpha_2} & \begin{matrix}0 & 0\\ 0 & 0\end{matrix} & & \dfrac{\left(\overline{\alpha}_1+\delta_1^B\right)\overline{M}_1}{\gamma_1} & -\dfrac{\left(\overline{\alpha}_2+\delta_2^B\right)\overline{M}_2}{\gamma_2}\end{bmatrix}=\begin{bmatrix}\mathbf{A} & \mathbf{B} & \mathbf{C}\\ \mathbf{D} & \mathbf{E} & \mathbf{F}\\ \mathbf{G} & \mathbf{H} & \mathbf{K}\end{bmatrix}\tag{17a}$$

$$\mathbf{N}\approx\begin{bmatrix}\alpha_1 p & -\alpha_2 p & \cos j_1 & -\cos j_2 & \gamma_1 p & -\gamma_2 p\\ \rho_1\alpha_1\left(1-2\beta_1^2p^2\right) & -\rho_2\alpha_2\left(1-2\beta_2^2p^2\right) & -2\rho_1\beta_1^2 p\cos j_1 & 2\rho_2\beta_2^2 p\cos j_2 & \rho_1\gamma_1\left(1-2\beta_1^2p^2\right) & -\rho_2\gamma_2\left(1-2\beta_2^2p^2\right)\\ \cos i_1 & \cos i_2 & -\beta_1 p & -\beta_2 p & 1 & 1\\ 2\rho_1\beta_1^2 p\cos i_1 & 2\rho_2\beta_2^2 p\cos i_2 & \rho_1\beta_1\left(1-2\beta_1^2p^2\right) & \rho_2\beta_2\left(1-2\beta_2^2p^2\right) & 2\rho_1\beta_1^2 p & 2\rho_2\beta_2^2 p\\ 0 & 0 & & & \delta_1^B & \delta_2^B\\ -\dfrac{\overline{\alpha}_1\overline{M}_1}{\alpha_1} & \dfrac{\overline{\alpha}_2\overline{M}_2}{\alpha_2} & \begin{matrix}0 & 0\\ 0 & 0\end{matrix} & & -\dfrac{\left(\overline{\alpha}_1+\delta_1^B\right)\overline{M}_1}{\gamma_1} & \dfrac{\left(\overline{\alpha}_2+\delta_2^B\right)\overline{M}_2}{\gamma_2}\end{bmatrix}=\begin{bmatrix}-\mathbf{A} & -\mathbf{B} & -\mathbf{C}\\ \mathbf{D} & \mathbf{E} & \mathbf{F}\\ -\mathbf{G} & -\mathbf{H} & \mathbf{K}'\end{bmatrix}\tag{17b}$$

$$\begin{bmatrix}\langle\mathbf{1}\rangle & \langle\mathbf{2}\rangle & \langle\mathbf{3}\rangle\\ \langle\mathbf{4}\rangle & \langle\mathbf{5}\rangle & \langle\mathbf{6}\rangle\\ \langle\mathbf{7}\rangle & \langle\mathbf{8}\rangle & \langle\mathbf{9}\rangle\end{bmatrix}=\begin{bmatrix}\mathbf{A} & \mathbf{B} & \mathbf{C}\\ \mathbf{D} & \mathbf{E} & \mathbf{F}\\ \mathbf{G} & \mathbf{H} & \mathbf{K}\end{bmatrix}^{-1}\begin{bmatrix}-\mathbf{A} & -\mathbf{B} & -\mathbf{C}\\ \mathbf{D} & \mathbf{E} & \mathbf{F}\\ -\mathbf{G} & -\mathbf{H} & \mathbf{K}'\end{bmatrix}\tag{17c}$$

where,

$$\langle\mathbf{1}\rangle=\begin{bmatrix}\overrightarrow{P}\overleftarrow{P} & \overleftarrow{P}\overleftarrow{P}\\ \overrightarrow{P}\overrightarrow{P} & \overleftarrow{P}\overrightarrow{P}\end{bmatrix},\langle\mathbf{2}\rangle=\begin{bmatrix}\overrightarrow{S}\overleftarrow{P} & \overleftarrow{S}\overleftarrow{P}\\ \overrightarrow{S}\overrightarrow{P} & \overleftarrow{S}\overrightarrow{P}\end{bmatrix},\langle\mathbf{3}\rangle=\begin{bmatrix}\overrightarrow{B}\overleftarrow{P} & \overleftarrow{B}\overleftarrow{P}\\ \overrightarrow{B}\overrightarrow{P} & \overleftarrow{B}\overrightarrow{P}\end{bmatrix},\langle\mathbf{4}\rangle=\begin{bmatrix}\overrightarrow{P}\overleftarrow{S} & \overleftarrow{P}\overleftarrow{S}\\ \overrightarrow{P}\overrightarrow{S} & \overleftarrow{P}\overrightarrow{S}\end{bmatrix},$$
$$\langle\mathbf{5}\rangle=\begin{bmatrix}\overrightarrow{S}\overleftarrow{S} & \overleftarrow{S}\overleftarrow{S}\\ \overrightarrow{S}\overrightarrow{S} & \overleftarrow{S}\overrightarrow{S}\end{bmatrix},\langle\mathbf{6}\rangle=\begin{bmatrix}\overrightarrow{B}\overleftarrow{S} & \overleftarrow{B}\overleftarrow{S}\\ \overrightarrow{B}\overrightarrow{S} & \overleftarrow{B}\overrightarrow{S}\end{bmatrix},\langle\mathbf{7}\rangle=\begin{bmatrix}\overrightarrow{P}\overleftarrow{B} & \overleftarrow{P}\overleftarrow{B}\\ \overrightarrow{P}\overrightarrow{B} & \overleftarrow{P}\overrightarrow{B}\end{bmatrix},\langle\mathbf{8}\rangle=\begin{bmatrix}\overrightarrow{S}\overleftarrow{B} & \overleftarrow{S}\overleftarrow{B}\\ \overrightarrow{S}\overrightarrow{B} & \overleftarrow{S}\overrightarrow{B}\end{bmatrix},$$
$$\langle\mathbf{9}\rangle=\begin{bmatrix}\overrightarrow{B}\overleftarrow{B} & \overleftarrow{B}\overleftarrow{B}\\ \overrightarrow{B}\overrightarrow{B} & \overleftarrow{B}\overrightarrow{B}\end{bmatrix}$$

$$\mathbf{A}=\begin{bmatrix}-\alpha_1 p & \alpha_2 p\\ -\rho_1\alpha_1\left(1-2\beta_1^2p^2\right) & \rho_2\alpha_2\left(1-2\beta_2^2p^2\right)\end{bmatrix},$$
$$\mathbf{B}=\begin{bmatrix}-\cos j_1 & \cos j_2\\ 2\rho_1\beta_1^2 p\cos j_1 & -2\rho_2\beta_2^2 p\cos j_2\end{bmatrix},$$
$$\mathbf{C}=\begin{bmatrix}-\gamma_1 p & \gamma_2 p\\ -\rho_1\gamma_1\left(1-2\beta_1^2p^2\right) & \rho_2\gamma_2\left(1-2\beta_2^2p^2\right)\end{bmatrix},$$
$$\mathbf{D}=\begin{bmatrix}\cos i_1 & \cos i_2\\ 2\rho_1\beta_1^2 p\cos i_1 & 2\rho_2\beta_2^2 p\cos i_2\end{bmatrix},$$
$$\mathbf{E}=\begin{bmatrix}-\beta_1 p & -\beta_2 p\\ \rho_1\beta_1\left(1-2\beta_1^2p^2\right) & \rho_2\beta_2\left(1-2\beta_2^2p^2\right)\end{bmatrix},\ \mathbf{F}=\begin{bmatrix}1 & 1\\ 2\rho_1\beta_1^2 p & 2\rho_2\beta_2^2 p\end{bmatrix},$$

$$\mathbf{G}=\begin{bmatrix}\dfrac{0}{\overline{\alpha}_1\overline{M}_1} & \dfrac{0}{-\overline{\alpha}_2\overline{M}_2}\\ \alpha_1 & \alpha_2\end{bmatrix},\quad \mathbf{H}=\begin{bmatrix}0 & 0\\ 0 & 0\end{bmatrix},\ \mathbf{K}=\begin{bmatrix}\delta_1^B & \delta_2^B\\ \dfrac{\left(\overline{\alpha}_1+\delta_1^B\right)\overline{M}_1}{\gamma_1} & -\dfrac{\left(\overline{\alpha}_2+\delta_2^B\right)\overline{M}_2}{\gamma_2}\end{bmatrix},$$
$$\mathbf{K}'=\begin{bmatrix}\delta_1^B & \delta_2^B\\ -\dfrac{\left(\overline{\alpha}_1+\delta_1^B\right)\overline{M}_1}{\gamma_1} & \dfrac{\left(\overline{\alpha}_2+\delta_2^B\right)\overline{M}_2}{\gamma_2}\end{bmatrix},\ \text{set}:\ \mathbf{K}''=\mathbf{K}+\mathbf{K}'=2\begin{bmatrix}\delta_1^B & \delta_2^B\\ 0 & 0\end{bmatrix}$$

3. Exact analytical expressions

Taking full account of the parameter symmetry of the coefficient matrix in Eqs. (17a) and (17b), the scattering coefficient in 17(c) can be solved, as shown in Eq. (18) (Eq. B-9). See Appendix B for the detailed solution process.

In Eq. (18), the submatrices ⟨**4**⟩ and ⟨**7**⟩ can be described independently by sub block matrices $\mathbf{A}\sim\mathbf{E}$ and their combinations; The submatrices ⟨**8**⟩ and ⟨**9**⟩ can be expressed as a linear combination of submatrix ⟨**7**⟩, and the submatrices ⟨**5**⟩ and ⟨**6**⟩ are linear combinations of submatrix ⟨**4**⟩; Finally, the submatrices ⟨**1**⟩, ⟨**2**⟩, and ⟨**3**⟩ can be written as linear combinations of submatrices ⟨**4**⟩ and⟨**7**⟩, ⟨**5**⟩ and⟨**8**⟩, ⟨**6**⟩ and⟨**9**⟩, respectively. This linear combination form shows that we can use sub block matrices $\mathbf{A}\sim\mathbf{E}$ and their combination to independently describe the scattering coefficient submatrices $\langle\mathbf{1}\rangle\sim\langle\mathbf{9}\rangle$, which means that the Exact Analytical Expressions of 36 scattering coefficients in equation (16) can be obtained by independently solving submatrices $\langle\mathbf{1}\rangle\sim\langle\mathbf{9}\rangle$.

Table 2(a)
Displacement vectors of scattered wave generated by incident fast P-wave from upper medium.

Medium	Type	Displacement
Upper medium	Upgoing *P*	$S(\sin i_1 \quad 0 \quad -\cos i_1)\overleftarrow{P}\overrightarrow{P}\exp\left[i\omega\left(px-\frac{\cos i_1}{\alpha_1}z-t\right)\right]$
	Upgoing *SV*	$S(\cos j_1 \quad 0 \quad \sin j_1)\overleftarrow{P}\overrightarrow{S}\exp\left[i\omega\left(px-\frac{\cos j_1}{\beta_1}z-t\right)\right]$
	Upgoing *B*	$S(\sin k_1 \quad 0 \quad -\cos k_1)\overleftarrow{P}\overrightarrow{B}\exp\left[i\omega\left(px-\frac{\cos k_1}{\gamma_1}z-t\right)\right]$
Lower medium	Downgoing *P*	$S(\sin i_2 \quad 0 \quad \cos i_2)\overrightarrow{P}\overrightarrow{P}\exp\left[i\omega\left(px+\frac{\cos i_2}{\alpha_2}z-t\right)\right]$
	Downgoing *SV*	$S(\cos j_2 \quad 0 \quad -\sin j_2)\overrightarrow{P}\overrightarrow{S}\exp\left[i\omega\left(px+\frac{\cos j_2}{\beta_2}z-t\right)\right]$
	Downgoing *B*	$S(\sin k_2 \quad 0 \quad \cos k_2)\overrightarrow{P}\overrightarrow{B}\exp\left[i\omega\left(px+\frac{\cos k_2}{\gamma_2}z-t\right)\right]$

Table 2(b)
Displacement vectors of scattered wave generated by incident fast P-wave from lower medium.

Medium	Type	Displacement
Upper medium	Upgoing *P*	$S(\sin i_1 \quad 0 \quad -\cos i_1)\overleftarrow{P}\overleftarrow{P}\exp\left[i\omega\left(px-\frac{\cos i_1}{\alpha_1}z-t\right)\right]$
	Upgoing *SV*	$S(\cos j_1 \quad 0 \quad \sin j_1)\overleftarrow{P}\overleftarrow{S}\exp\left[i\omega\left(px-\frac{\cos j_1}{\beta_1}z-t\right)\right]$
	Upgoing *B*	$S(\sin k_1 \quad 0 \quad -\cos k_1)\overleftarrow{P}\overleftarrow{B}\exp\left[i\omega\left(px-\frac{\cos k_1}{\gamma_1}z-t\right)\right]$
Lower medium	Downgoing *P*	$S(\sin i_2 \quad 0 \quad \cos i_2)\overleftarrow{P}\overrightarrow{P}\exp\left[i\omega\left(px+\frac{\cos i_2}{\alpha_2}z-t\right)\right]$
	Downgoing *SV*	$S(\cos j_2 \quad 0 \quad -\sin j_2)\overleftarrow{P}\overrightarrow{S}\exp\left[i\omega\left(px+\frac{\cos j_2}{\beta_2}z-t\right)\right]$
	Downgoing B	$S(\sin k_2 \quad 0 \quad \cos k_2)\overleftarrow{P}\overrightarrow{B}\exp\left[i\omega\left(px+\frac{\cos k_2}{\gamma_2}z-t\right)\right]$

Table 2(c)
Displacement vectors of scattered wave generated by incident SV-wave from upper medium.

Medium	Type	Displacement
Upper medium	*Upgoing P*	$S(\sin i_1 \quad 0 \quad -\cos i_1)\overleftarrow{S}\overrightarrow{P}\exp\left[i\omega\left(px-\frac{\cos i_1}{\alpha_1}z-t\right)\right]$
	Upgoing SV	$S(\cos j_1 \quad 0 \quad \sin j_1)\overleftarrow{S}\overleftarrow{S}\exp\left[i\omega\left(px-\frac{\cos j_1}{\beta_1}z-t\right)\right]$
	Upgoing B	$S(\sin k_1 \quad 0 \quad -\cos k_1)\overleftarrow{S}\overleftarrow{B}\exp\left[i\omega\left(px-\frac{\cos k_1}{\gamma_1}z-t\right)\right]$
Lower medium	*Downgoing P*	$S(\sin i_2 \quad 0 \quad \cos i_2)\overleftarrow{S}\overrightarrow{P}\exp\left[i\omega\left(px+\frac{\cos i_2}{\alpha_2}z-t\right)\right]$
	Downgoing SV	$S(\cos j_2 \quad 0 \quad -\sin j_2)\overleftarrow{S}\overrightarrow{S}\exp\left[i\omega\left(px+\frac{\cos j_2}{\beta_2}z-t\right)\right]$
	Downgoing B	$S(\sin k_2 \quad 0 \quad \cos k_2)\overleftarrow{S}\overrightarrow{B}\exp\left[i\omega\left(px+\frac{\cos k_2}{\gamma_2}z-t\right)\right]$

Table 2(d)
Displacement vectors of scattered wave generated by incident SV-wave from lower medium.

Medium	Type	Displacement
Upper medium	Upgoing *P*	$S(\sin i_1 \quad 0 \quad -\cos i_1)\overleftarrow{S}\overleftarrow{P}\exp\left[i\omega\left(px-\frac{\cos i_1}{\alpha_1}z-t\right)\right]$
	Upgoing *SV*	$S(\cos j_1 \quad 0 \quad \sin j_1)\overleftarrow{S}\overleftarrow{S}\exp\left[i\omega\left(px-\frac{\cos j_1}{\beta_1}z-t\right)\right]$
	Upgoing *B*	$S(\sin k_1 \quad 0 \quad -\cos k_1)\overleftarrow{S}\overleftarrow{B}\exp\left[i\omega\left(px-\frac{\cos k_1}{\gamma_1}z-t\right)\right]$
Lower medium	Downgoing *P*	$S(\sin i_2 \quad 0 \quad \cos i_2)\overleftarrow{S}\overrightarrow{P}\exp\left[i\omega\left(px+\frac{\cos i_2}{\alpha_2}z-t\right)\right]$
	Downgoing *SV*	$S(\cos j_2 \quad 0 \quad -\sin j_2)\overleftarrow{S}\overrightarrow{S}\exp\left[i\omega\left(px+\frac{\cos j_2}{\beta_2}z-t\right)\right]$
	Downgoing B	$S(\sin k_2 \quad 0 \quad \cos k_2)\overleftarrow{S}\overrightarrow{B}\exp\left[i\omega\left(px+\frac{\cos k_2}{\gamma_2}z-t\right)\right]$

$$\begin{bmatrix} \langle \mathbf{1} \rangle & \langle \mathbf{2} \rangle & \langle \mathbf{3} \rangle \\ \langle \mathbf{4} \rangle & \langle \mathbf{5} \rangle & \langle \mathbf{6} \rangle \\ \langle \mathbf{7} \rangle & \langle \mathbf{8} \rangle & \langle \mathbf{9} \rangle \end{bmatrix} =$$

$$\begin{bmatrix} -\left\{\mathbf{I}+\mathbf{A}^{-1}\mathbf{B}\cdot\langle \mathbf{4} \rangle+\mathbf{A}^{-1}\mathbf{C}\cdot\langle \mathbf{7} \rangle\right\} & -\left\{\mathbf{A}^{-1}\mathbf{B}(\mathbf{I}+\langle \mathbf{5} \rangle)+\mathbf{A}^{-1}\mathbf{C}\cdot\langle \mathbf{8} \rangle\right\} & -\left\{\mathbf{A}^{-1}\mathbf{B}\cdot\langle \mathbf{6} \rangle+\mathbf{A}^{-1}\mathbf{C}\cdot(\mathbf{I}+\langle \mathbf{9} \rangle)\right\} \\ 2\mathbf{S}_{11}\mathbf{V}_2 & \frac{1}{2}\cdot\langle \mathbf{4} \rangle\cdot\left(\mathbf{A}^{-1}\mathbf{B}+\mathbf{D}^{-1}\mathbf{E}\right)-\mathbf{S}_{11}\mathbf{G}\mathbf{A}^{-1}\mathbf{B} & \mathbf{S}_{11}\left(2\mathbf{V}_2\mathbf{D}^{-1}\mathbf{F}-\mathbf{K}''\right)=\langle \mathbf{4} \rangle\cdot\mathbf{D}^{-1}\mathbf{F}-\mathbf{S}_{11}\mathbf{K}'' \\ 2\mathbf{S}_{21}\mathbf{V}_1 & \langle \mathbf{7} \rangle\cdot\mathbf{D}^{-1}\mathbf{E} & \frac{1}{2}\cdot\langle \mathbf{7} \rangle\cdot\left(\mathbf{A}^{-1}\mathbf{C}+\mathbf{D}^{-1}\mathbf{F}\right)+\mathbf{S}_{21}\left(\mathbf{G}\mathbf{A}^{-1}\mathbf{C}+\mathbf{K}'\right) \end{bmatrix} \tag{18}$$

Solving two-dimensional (2D) submatrices $\mathbf{A}\sim\mathbf{E}$ and their composite forms step by step (Appendix C), and substituting the results into Eq. (18), the analytical solutions of 36 scattering coefficients are finally derived as,

$$\begin{bmatrix} \overleftarrow{P}\overrightarrow{B} & \overrightarrow{P}\overrightarrow{B} \\ \overleftarrow{P}\overleftarrow{B} & \overrightarrow{P}\overleftarrow{B} \end{bmatrix} = -\frac{2gh\cdot\alpha_1\alpha_2}{\bar{X}(\tilde{\Delta}+\tilde{\nabla})}\begin{bmatrix} \left(\tilde{R}\frac{\cos j_1}{\beta_1}+\tilde{H}\frac{\cos j_2}{\beta_2}\right)\delta_2^B\cos i_1 & \left(\tilde{G}\frac{\cos j_1}{\beta_1}+\tilde{Q}\frac{\cos j_2}{\beta_2}\right)\delta_2^B\cos i_2 \\ -\left(\tilde{R}\frac{\cos j_1}{\beta_1}+\tilde{H}\frac{\cos j_2}{\beta_2}\right)\delta_1^B\cos i_1 & -\left(\tilde{G}\frac{\cos j_1}{\beta_1}+\tilde{Q}\frac{\cos j_2}{\beta_2}\right)\delta_1^B\cos i_2 \end{bmatrix} \tag{19}$$

$$\begin{bmatrix} \overleftarrow{S}\overrightarrow{B} & \overrightarrow{S}\overrightarrow{B} \\ \overleftarrow{S}\overleftarrow{B} & \overrightarrow{S}\overleftarrow{B} \end{bmatrix} = -\frac{1}{\cos i_1\cos i_2\cdot p\cdot d}\begin{bmatrix} \beta_1\left(\overleftarrow{P}\overrightarrow{B}\cdot c\cos i_2-\overrightarrow{P}\overrightarrow{B}\cdot\rho_1\cos i_1\right) & \beta_2\left(\overleftarrow{P}\overrightarrow{B}\cdot\rho_2\cos i_2-\overrightarrow{P}\overrightarrow{B}\cdot b\cos i_1\right) \\ \beta_1\left(\overleftarrow{P}\overleftarrow{B}\cdot c\cos i_2-\overrightarrow{P}\overleftarrow{B}\cdot\rho_1\cos i_1\right) & \beta_2\left(\overleftarrow{P}\overleftarrow{B}\cdot\rho_2\cos i_2-\overrightarrow{P}\overleftarrow{B}\cdot b\cos i_1\right) \end{bmatrix} \tag{20}$$

$$\begin{bmatrix} \overleftarrow{B}\overrightarrow{B} & \overrightarrow{B}\overrightarrow{B} \\ \overleftarrow{B}\overleftarrow{B} & \overrightarrow{B}\overleftarrow{B} \end{bmatrix} = \frac{1}{2\cos i_1\cos i_2}\begin{bmatrix} \overleftarrow{P}\overrightarrow{B}\cdot\left(1+\gamma_1\frac{\cos i_1}{\alpha_1}\right)\cos i_2 & \overrightarrow{P}\overrightarrow{B}\cdot\left(1+\gamma_2\frac{\cos i_2}{\alpha_2}\right)\cos i_1 \\ \overleftarrow{P}\overleftarrow{B}\cdot\left(1+\gamma_1\frac{\cos i_1}{\alpha_1}\right)\cos i_2 & \overrightarrow{P}\overleftarrow{B}\cdot\left(1+\gamma_2\frac{\cos i_2}{\alpha_2}\right)\cos i_1 \end{bmatrix} + \frac{1}{\tilde{\Delta}+\tilde{\nabla}}\begin{bmatrix} h\alpha_1\left(\tilde{V}\delta_1^B-\frac{\overline{U}}{\gamma_1}g\alpha_2\delta_2^B\right) & h\alpha_1\left(\tilde{V}+\frac{\overline{V}}{\gamma_2}g\alpha_2\right)\delta_2^B \\ g\alpha_2\left(\tilde{U}+\frac{\overline{U}}{\gamma_1}h\alpha_1\right)\delta_1^B & g\alpha_2\left(\tilde{U}\delta_2^B-\frac{\overline{V}}{\gamma_2}h\alpha_1\delta_1^B\right) \end{bmatrix} \tag{21}$$

$$\begin{bmatrix} \overleftarrow{P}\overrightarrow{S} & \overrightarrow{P}\overrightarrow{S} \\ \overleftarrow{P}\overleftarrow{S} & \overrightarrow{P}\overleftarrow{S} \end{bmatrix} = \frac{2ap}{\bar{X}(\tilde{\Delta}+\tilde{\nabla})}\cdot\begin{bmatrix} \frac{1}{\beta_1}(\overline{R}\cdot\tilde{M}+\rho_2\overline{G}\cdot\tilde{N})h\alpha_1\cos i_1 & \frac{1}{\beta_1}(\overline{R}\cdot\tilde{O}+\rho_2\overline{G}\cdot\tilde{P})g\alpha_2\cos i_2 \\ -\frac{1}{\beta_2}(\rho_1\overline{H}\cdot\tilde{M}+\overline{Q}\cdot\tilde{N})h\alpha_1\cos i_1 & -\frac{1}{\beta_2}(\rho_1\overline{H}\cdot\tilde{O}+\overline{Q}\cdot\tilde{P})g\alpha_2\cos i_2 \end{bmatrix} \tag{22}$$

$$\begin{bmatrix} \overleftarrow{S}\overleftarrow{S} & \overrightarrow{S}\overleftarrow{S} \\ \overleftarrow{S}\overrightarrow{S} & \overrightarrow{S}\overrightarrow{S} \end{bmatrix} = -\frac{\beta_1\beta_2}{2adp\cdot\cos i_1\cos i_2}\cdot\begin{bmatrix} \frac{1}{\beta_2}\left(\overleftarrow{P}\overrightarrow{S}\cdot\overline{Q}'\cos i_2-\overrightarrow{P}\overrightarrow{S}\cdot\rho_1\overline{H}'\cos i_1\right) & \frac{1}{\beta_1}\left(\overleftarrow{P}\overrightarrow{S}\cdot\rho_2\overline{G}'\cos i_2-\overrightarrow{P}\overrightarrow{S}\cdot\overline{R}'\cos i_1\right) \\ \frac{1}{\beta_2}\left(\overleftarrow{P}\overleftarrow{S}\cdot\overline{Q}'\cos i_2-\overrightarrow{P}\overleftarrow{S}\cdot\rho_1\overline{H}'\cos i_1\right) & \frac{1}{\beta_1}\left(\overleftarrow{P}\overleftarrow{S}\cdot\rho_2\overline{G}'\cos i_2-\overrightarrow{P}\overleftarrow{S}\cdot\overline{R}'\cos i_1\right) \end{bmatrix} + \frac{gh}{\bar{X}(\tilde{\Delta}+\tilde{\nabla})}\cdot\begin{bmatrix} \tilde{A}(l\rho_1-sb)\frac{\cos j_1}{\beta_1} & -\tilde{A}(lc-s\rho_2)\frac{\cos j_2}{\beta_1} \\ -\tilde{B}(l\rho_1-sb)\frac{\cos j_1}{\beta_2} & \tilde{B}(lc-s\rho_2)\frac{\cos j_2}{\beta_2} \end{bmatrix} \tag{23}$$

$$\begin{bmatrix} \overleftarrow{B}\overrightarrow{S} & \overrightarrow{B}\overrightarrow{S} \\ \overleftarrow{B}\overleftarrow{S} & \overrightarrow{B}\overleftarrow{S} \end{bmatrix} = \frac{1}{\cos i_1\cos i_2}\begin{bmatrix} \overleftarrow{P}\overrightarrow{S}\cdot\cos i_2 & \overrightarrow{P}\overrightarrow{S}\cdot\cos i_1 \\ \overleftarrow{P}\overleftarrow{S}\cdot\cos i_2 & \overrightarrow{P}\overleftarrow{S}\cdot\cos i_1 \end{bmatrix} - \frac{2ap\cdot gh}{\bar{X}(\tilde{\Delta}+\tilde{\nabla})}\begin{bmatrix} \frac{\delta_1^B}{\beta_1}(\overline{R}\tilde{V}+\rho_2\overline{G}\tilde{U}) & \frac{\delta_2^B}{\beta_1}(\overline{R}\tilde{V}+\rho_2\overline{G}\tilde{U}) \\ -\frac{\delta_1^B}{\beta_2}(\rho_1\overline{H}\tilde{V}+\overline{Q}\tilde{U}) & -\frac{\delta_2^B}{\beta_2}(\rho_1\overline{H}\tilde{V}+\overline{Q}\tilde{U}) \end{bmatrix} \tag{24}$$

$$\begin{bmatrix} \overleftarrow{P}\overleftarrow{P} & \overrightarrow{P}\overleftarrow{P} \\ \overleftarrow{P}\overrightarrow{P} & \overrightarrow{P}\overrightarrow{P} \end{bmatrix} = -\frac{1}{p\cdot a}\begin{bmatrix} \frac{1}{\alpha_1}\cdot\left(\overleftarrow{P}\overrightarrow{S}\cdot b\cos j_1-\overleftarrow{P}\overleftarrow{S}\cdot\rho_2\cos j_2\right) & \frac{1}{\alpha_1}\cdot\left(\overrightarrow{P}\overrightarrow{S}\cdot b\cos j_1-\overrightarrow{P}\overleftarrow{S}\cdot\rho_2\cos j_2\right) \\ \frac{1}{\alpha_2}\cdot\left(\overleftarrow{P}\overrightarrow{S}\cdot\rho_1\cos j_1-\overleftarrow{P}\overleftarrow{S}\cdot c\cos j_2\right) & \frac{1}{\alpha_2}\cdot\left(\overrightarrow{P}\overrightarrow{S}\cdot\rho_1\cos j_1-\overrightarrow{P}\overleftarrow{S}\cdot c\cos j_2\right) \end{bmatrix} - \begin{bmatrix} 1+\overleftarrow{P}\overrightarrow{B}\cdot\frac{\gamma_1}{\alpha_1} & \overrightarrow{P}\overrightarrow{B}\cdot\frac{\gamma_1}{\alpha_1} \\ \overleftarrow{P}\overleftarrow{B}\cdot\frac{\gamma_2}{\alpha_2} & 1+\overrightarrow{P}\overleftarrow{B}\cdot\frac{\gamma_2}{\alpha_2} \end{bmatrix} \tag{25}$$

$$\begin{bmatrix} \overleftarrow{S}\overleftarrow{P} & \overrightarrow{S}\overleftarrow{P} \\ \overleftarrow{S}\overrightarrow{P} & \overrightarrow{S}\overrightarrow{P} \end{bmatrix} = -\frac{1}{pa}\begin{bmatrix} \frac{1}{\alpha_1}\left[\left(1+\overleftarrow{S}\overrightarrow{S}\right)\cdot b\cos j_1-\overleftarrow{S}\overleftarrow{S}\cdot\rho_2\cos j_2\right] & \frac{1}{\alpha_1}\left[\overrightarrow{S}\overrightarrow{S}\cdot b\cos j_1-\left(1+\overrightarrow{S}\overleftarrow{S}\right)\cdot\rho_2\cos j_2\right] \\ \frac{1}{\alpha_2}\left[\left(1+\overleftarrow{S}\overrightarrow{S}\right)\cdot\rho_1\cos j_1-\overleftarrow{S}\overleftarrow{S}\cdot c\cos j_2\right] & \frac{1}{\alpha_2}\left[\overrightarrow{S}\overrightarrow{S}\cdot\rho_1\cos j_1-\left(1+\overrightarrow{S}\overleftarrow{S}\right)\cdot c\cos j_2\right] \end{bmatrix} - \begin{bmatrix} \overleftarrow{S}\overrightarrow{B}\cdot\frac{\gamma_1}{\alpha_1} & \overrightarrow{S}\overrightarrow{B}\cdot\frac{\gamma_1}{\alpha_1} \\ \overleftarrow{S}\overleftarrow{B}\cdot\frac{\gamma_2}{\alpha_2} & \overrightarrow{S}\overleftarrow{B}\cdot\frac{\gamma_2}{\alpha_2} \end{bmatrix} \tag{26}$$

$$\begin{bmatrix} \overleftarrow{B}\overleftarrow{P} & \overrightarrow{B}\overleftarrow{P} \\ \overleftarrow{B}\overrightarrow{P} & \overrightarrow{B}\overrightarrow{P} \end{bmatrix} = -\frac{1}{p\cdot a}\begin{bmatrix} \frac{1}{\alpha_1}\left(\overleftarrow{B}\overrightarrow{S}\cdot b\cos j_1-\overleftarrow{B}\overleftarrow{S}\cdot\rho_2\cos j_2\right) & \frac{1}{\alpha_1}\left(\overrightarrow{B}\overrightarrow{S}\cdot b\cos j_1-\overrightarrow{B}\overleftarrow{S}\cdot\rho_2\cos j_2\right) \\ \frac{1}{\alpha_2}\left(\overleftarrow{B}\overrightarrow{S}\cdot\rho_1\cos j_1-\overleftarrow{B}\overleftarrow{S}\cdot c\cos j_2\right) & \frac{1}{\alpha_2}\left(\overrightarrow{B}\overrightarrow{S}\cdot\rho_1\cos j_1-\overrightarrow{B}\overleftarrow{S}\cdot c\cos j_2\right) \end{bmatrix} - \begin{bmatrix} \left(1+\overleftarrow{B}\overrightarrow{B}\right)\cdot\frac{\gamma_1}{\alpha_1} & \overrightarrow{B}\overrightarrow{B}\cdot\frac{\gamma_1}{\alpha_1} \\ \overleftarrow{B}\overleftarrow{B}\cdot\frac{\gamma_2}{\alpha_2} & \left(1+\overrightarrow{B}\overleftarrow{B}\right)\cdot\frac{\gamma_2}{\alpha_2} \end{bmatrix} \tag{27}$$

Table 2(e)
Displacement vectors of scattered wave generated by incident slow P-wave from upper medium.

Medium	Type	Displacement
Upper medium	Upgoing *P*	$S(\sin i_1 \quad 0 \quad -\cos i_1)\overset{\searrow}{B}\overset{\nearrow}{P}\exp\left[i\omega\left(px-\frac{\cos i_1}{\alpha_1}z-t\right)\right]$
	Upgoing *SV*	$S(\cos j_1 \quad 0 \quad \sin j_1)\overset{\searrow}{B}\overset{\nearrow}{S}\exp\left[i\omega\left(px-\frac{\cos j_1}{\beta_1}z-t\right)\right]$
	Upgoing *B*	$S(\sin k_1 \quad 0 \quad -\cos k_1)\overset{\searrow}{B}\overset{\nearrow}{B}\exp\left[i\omega\left(px-\frac{\cos k_1}{\gamma_1}z-t\right)\right]$
Lower medium	Downgoing *P*	$S(\sin i_2 \quad 0 \quad \cos i_2)\overset{\searrow}{B}\overset{\searrow}{P}\exp\left[i\omega\left(px+\frac{\cos i_2}{\alpha_2}z-t\right)\right]$
	Downgoing *SV*	$S(\cos j_2 \quad 0 \quad -\sin j_2)\overset{\searrow}{B}\overset{\searrow}{S}\exp\left[i\omega\left(px+\frac{\cos j_2}{\beta_2}z-t\right)\right]$
	Downgoing B	$S(\sin k_2 \quad 0 \quad \cos k_2)\overset{\searrow}{B}\overset{\searrow}{B}\exp\left[i\omega\left(px+\frac{\cos k_2}{\gamma_2}z-t\right)\right]$

Table 2(f)
Displacement vectors of scattered wave generated by incident slow P-wave from lower medium.

Medium	Type	Displacement
Upper medium	Upgoing *P*	$S(\sin i_1 \quad 0 \quad -\cos i_1)\overset{\nearrow}{B}\overset{\nearrow}{P}\exp\left[i\omega\left(px-\frac{\cos i_1}{\alpha_1}z-t\right)\right]$
	Upgoing *SV*	$S(\cos j_1 \quad 0 \quad \sin j_1)\overset{\nearrow}{B}\overset{\nearrow}{S}\exp\left[i\omega\left(px-\frac{\cos j_1}{\beta_1}z-t\right)\right]$
	Upgoing *B*	$S(\sin k_1 \quad 0 \quad -\cos k_1)\overset{\nearrow}{B}\overset{\nearrow}{B}\exp\left[i\omega\left(px-\frac{\cos k_1}{\gamma_1}z-t\right)\right]$
Lower medium	Downgoing *P*	$S(\sin i_2 \quad 0 \quad \cos i_2)\overset{\nearrow}{B}\overset{\searrow}{P}\exp\left[i\omega\left(px+\frac{\cos i_2}{\alpha_2}z-t\right)\right]$
	Downgoing *SV*	$S(\cos j_2 \quad 0 \quad -\sin j_2)\overset{\nearrow}{B}\overset{\searrow}{S}\exp\left[i\omega\left(px+\frac{\cos j_2}{\beta_2}z-t\right)\right]$
	Downgoing B	$S(\sin k_2 \quad 0 \quad \cos k_2)\overset{\nearrow}{B}\overset{\searrow}{B}\exp\left[i\omega\left(px+\frac{\cos k_2}{\gamma_2}z-t\right)\right]$

In Eqs. (19)–(27), the expression forms of some parameters are similar to Aki and Richards (1980) (Table C-1), and others are related to pores and pore fluids (Table C-2). The expression forms of Eqs. (19)–(27) realizes the ability to independently describe any scattering coefficient by using properties of rock, pore, and its fluids of upper and lower media. They decouple 36 scattering coefficients from scattering matrix (Eq. (18)), which avoids mutual interference between various scattering coefficients.

4. Approximate analytical expressions

There is a nonlinear relationship between the resolved scattering coefficients and the parameters of rock, pore, and its fluids in Eqs. (19)–(27), which is difficult to be applied in practical production. Under the assumptions of weak elasticity and small angle incidence at the interface of porous media, we first make an approximate transformation of the relevant parameters in Eqs. (19)–(27). See Appendix D for the detailed process.

With the first- and second-order approximations of the relevant parameters in Table C-1 and C-2 being substituted into the exact analytical expressions (Eqs. (19)–(27)), and ignoring the second- and above-order items of final results, the first-order approximate expressions of 36 scattering coefficients, which can be described by the fast P-wave velocity, SV-wave velocity, slow P-wave velocity, equivalent density, Biot's parameters, and displacement amplitude ratio corresponding to the slow P-wave are derived as,

$$\begin{bmatrix} \overset{\searrow}{P}\overset{\nearrow}{B} & \overset{\nearrow}{P}\overset{\nearrow}{B} \\ \overset{\searrow}{P}\overset{\searrow}{B} & \overset{\nearrow}{P}\overset{\searrow}{B} \end{bmatrix} \approx \frac{\gamma}{2\rho\alpha}\cdot\frac{\overline{\alpha}}{\overline{\alpha}+\delta^B}(-a+\rho\overline{Z})\begin{bmatrix} 1 & 1 \\ -1 & -1 \end{bmatrix}, \tag{28}$$

$$\begin{bmatrix} \overset{\searrow}{S}\overset{\nearrow}{B} & \overset{\nearrow}{S}\overset{\nearrow}{B} \\ \overset{\searrow}{S}\overset{\searrow}{B} & \overset{\nearrow}{S}\overset{\searrow}{B} \end{bmatrix} \approx \frac{\beta\gamma}{2\rho\alpha^2}\cdot\frac{\overline{\alpha}}{\overline{\alpha}+\delta^B}dp\frac{\cos j}{\beta}\begin{bmatrix} 1 & 1 \\ -1 & -1 \end{bmatrix}, \tag{29}$$

$$\begin{bmatrix} \overset{\searrow}{B}\overset{\nearrow}{B} & \overset{\nearrow}{B}\overset{\nearrow}{B} \\ \overset{\searrow}{B}\overset{\searrow}{B} & \overset{\nearrow}{B}\overset{\searrow}{B} \end{bmatrix} \approx \begin{bmatrix} 0 & 1 \\ 1 & 0 \end{bmatrix} + \frac{\Delta\delta^B}{\delta^B}\begin{bmatrix} 0 & 1 \\ -1 & 0 \end{bmatrix} + \frac{1}{2}\left\{\frac{\Delta\overline{M}}{\overline{M}} - \frac{\Delta\gamma}{\gamma} + \frac{\overline{\alpha}}{\overline{\alpha}+\delta^B}\left[\frac{\Delta\overline{\alpha}}{\overline{\alpha}} - \frac{\Delta\delta^B}{\delta^B} + \left(\frac{\gamma}{\alpha}\right)^2\left(-\frac{a}{\rho}+\overline{Z}\right)\right]\right\}\begin{bmatrix} 1 & 1 \\ -1 & -1 \end{bmatrix} \tag{30}$$

$$\begin{bmatrix} \overset{\searrow}{P}\overset{\nearrow}{S} & \overset{\nearrow}{P}\overset{\nearrow}{S} \\ \overset{\searrow}{P}\overset{\searrow}{S} & \overset{\nearrow}{P}\overset{\searrow}{S} \end{bmatrix} \approx -\frac{\alpha p}{2\beta\rho\frac{\cos j}{\beta}}\left\{a\begin{bmatrix} 1 & 1 \\ -1 & -1 \end{bmatrix} + d\frac{\cos i}{\alpha}\frac{\cos j}{\beta}\begin{bmatrix} 1 & -1 \\ 1 & -1 \end{bmatrix}\right\} \tag{31}$$

$$\begin{bmatrix} \overset{\searrow}{S}\overset{\nearrow}{S} & \overset{\nearrow}{S}\overset{\nearrow}{S} \\ \overset{\searrow}{S}\overset{\searrow}{S} & \overset{\nearrow}{S}\overset{\searrow}{S} \end{bmatrix} \approx \begin{bmatrix} 0 & 1 \\ 1 & 0 \end{bmatrix} + \frac{1}{2}\left(\frac{d}{\rho}p^2 - \tan^2 j\frac{\Delta\beta}{\beta}\right)\begin{bmatrix} 1 & 1 \\ -1 & -1 \end{bmatrix} - \frac{1}{2}\left(\frac{a}{\rho}+\frac{\Delta\beta}{\beta}\right)\begin{bmatrix} 1 & -1 \\ 1 & -1 \end{bmatrix} \tag{32}$$

$$\begin{bmatrix} \overset{\searrow}{B}\overset{\nearrow}{S} & \overset{\nearrow}{B}\overset{\nearrow}{S} \\ \overset{\searrow}{B}\overset{\searrow}{S} & \overset{\nearrow}{B}\overset{\searrow}{S} \end{bmatrix} \approx -\frac{\alpha p}{2\rho\cos i\cos j}\left\{a\cdot\gamma\frac{\cos i}{\alpha}\begin{bmatrix} 1 & 1 \\ -1 & -1 \end{bmatrix} + d\frac{\cos i}{\alpha}\frac{\cos j}{\beta}\begin{bmatrix} 1 & -1 \\ 1 & -1 \end{bmatrix}\right\} \tag{33}$$

$$\begin{bmatrix} \overset{\searrow}{P}\overset{\nearrow}{P} & \overset{\nearrow}{P}\overset{\nearrow}{P} \\ \overset{\searrow}{P}\overset{\searrow}{P} & \overset{\nearrow}{P}\overset{\searrow}{P} \end{bmatrix} \approx \begin{bmatrix} 0 & 1 \\ 1 & 0 \end{bmatrix} + \frac{1}{2}\left(\tan^2 i\frac{\Delta\alpha}{\alpha} - \frac{d}{\rho}p^2\right) \times \begin{bmatrix} 1 & -1 \\ 1 & -1 \end{bmatrix} + \frac{1}{2}\left[\frac{\Delta\rho}{\rho} + \frac{\Delta\alpha}{\alpha} - \frac{d}{\rho}p^2 - \frac{\gamma^2}{\alpha^2}\cdot\frac{\overline{\alpha}}{\overline{\alpha}+\delta^B}\left(-\frac{a}{\rho}+\overline{Z}\right)\right]\begin{bmatrix} 1 & 1 \\ -1 & -1 \end{bmatrix} \tag{34}$$

$$\begin{bmatrix} \overset{\searrow}{S}\overset{\nearrow}{P} & \overset{\nearrow}{S}\overset{\nearrow}{P} \\ \overset{\searrow}{S}\overset{\searrow}{P} & \overset{\nearrow}{S}\overset{\searrow}{P} \end{bmatrix} \approx -\frac{\beta p}{2\rho\cos i}\left\{a\begin{bmatrix} 1 & -1 \\ 1 & -1 \end{bmatrix} + \left(1+\frac{\gamma^2}{\alpha^2}\cdot\frac{\overline{\alpha}}{\overline{\alpha}+\delta^B}\right)d\frac{\cos i}{\alpha}\frac{\cos j}{\beta}\begin{bmatrix} 1 & 1 \\ -1 & -1 \end{bmatrix}\right\} \tag{35}$$

$$\begin{bmatrix} \overset{\searrow}{B}\overset{\nearrow}{P} & \overset{\nwarrow}{B}\overset{\nearrow}{P} \\ \overset{\searrow}{B}\overset{\searrow}{P} & \overset{\nwarrow}{B}\overset{\searrow}{P} \end{bmatrix} \approx -\frac{1}{2\cos i}\left\{\frac{d}{\rho}p^2 - \frac{\Delta\delta^B}{\delta^B}\right\}\begin{bmatrix} 1 & -1 \\ 1 & -1 \end{bmatrix} + \frac{\gamma}{2\alpha}\left\{\frac{a}{\rho} + 2\frac{\Delta\gamma}{\gamma} - \frac{\Delta\overline{M}}{\overline{M}} - \frac{\Delta\overline{\alpha}+\Delta\delta^B}{\overline{\alpha}+\delta^B} - \left(\frac{\gamma}{\alpha}\right)^2 \cdot \frac{\overline{\alpha}}{\overline{\alpha}+\delta^B}\overline{Z}\right\}\begin{bmatrix} 1 & 1 \\ -1 & -1 \end{bmatrix} \tag{36}$$

here, $\overline{Z} = \frac{\Delta\overline{\alpha}}{\overline{\alpha}} + \frac{\Delta\overline{M}}{\overline{M}} - 2\frac{\Delta\alpha}{\alpha}$.

As the incident and scattering system of the constructed P-SV-B plane waves (Fig. 1) is symmetrical, the approximate expressions of the scattering coefficients in Eqs. (28)–(36) are also symmetrical, respectively. Taking Eq. (32) as an example, the constant terms of approximate expressions $\overset{\searrow}{S}\overset{\nearrow}{S}$ (SV-wave reflection coefficient with SV-wave being incident from upper porous medium) and $\overset{\nearrow}{S}\overset{\searrow}{S}$ (that from lower porous medium) are equal, and the coefficients of their first-order term differ by a negative sign, which is caused by the difference of wave propagation direction.

The first-order approximate expression of the ratio between the displacement amplitude of pore fluid relative to rock skeleton and that of rock skeleton corresponding to the slow P-wave δ^B (Eq. A-3c) can be expressed as,

$$\delta^B \approx -\frac{\rho\alpha^2}{\overline{\alpha}\overline{M}}, \tag{37a}$$

$$\frac{\Delta\delta^B}{\delta^B} \approx -\overline{Z} + \frac{\Delta\rho}{\rho}. \tag{37b}$$

here, the first-order term's coefficient of δ^B is zero.

Replace Eq. (37) into Eqs. (28)–(36), and considering the symmetry in Eqs. (28)–(36), the approximate expressions of scattering coefficients can be expressed as,

$$\begin{bmatrix} \overset{\searrow}{P}\overset{\nearrow}{B} \\ \overset{\searrow}{P}\overset{\searrow}{B} \end{bmatrix} \approx \frac{\gamma}{2\rho\alpha}\cdot\frac{\overline{\alpha}^2\overline{M}}{\overline{\alpha}^2\overline{M}-\rho\alpha^2}(-a+\rho\overline{Z})\begin{bmatrix} 1 \\ -1 \end{bmatrix}, \tag{38}$$

$$\begin{bmatrix} \overset{\searrow}{S}\overset{\nearrow}{B} \\ \overset{\searrow}{S}\overset{\searrow}{B} \end{bmatrix} \approx \frac{\beta\gamma}{2\rho\alpha^2}\frac{\overline{\alpha}^2\overline{M}}{\overline{\alpha}^2\overline{M}-\rho\alpha^2}dp\frac{\cos j}{\beta}\begin{bmatrix} 1 \\ -1 \end{bmatrix}, \tag{39}$$

$$\begin{bmatrix} \overset{\searrow}{B}\overset{\nearrow}{B} \\ \overset{\searrow}{B}\overset{\searrow}{B} \end{bmatrix} \approx \begin{bmatrix} 0 \\ 1 \end{bmatrix} + \frac{1}{2}\left(\overline{Z} - \frac{\Delta\rho}{\rho}\right)\begin{bmatrix} 1 \\ 1 \end{bmatrix} + \frac{1}{2}\left\{-\overline{Z} + \frac{\Delta\rho}{\rho} + \frac{\Delta\overline{M}}{\overline{M}} - \frac{\Delta\gamma}{\gamma} + \frac{\overline{\alpha}^2\overline{M}}{\overline{\alpha}^2\overline{M}-\rho\alpha^2}\left[\frac{\Delta\overline{\alpha}}{\overline{\alpha}} + \overline{Z} - \frac{\Delta\rho}{\rho} + \left(\frac{\gamma}{\alpha}\right)^2\cdot\frac{dp^2}{\rho}\right]\right\}\begin{bmatrix} 1 \\ -1 \end{bmatrix}, \tag{40}$$

$$\begin{bmatrix} \overset{\searrow}{P}\overset{\nearrow}{S} \\ \overset{\searrow}{P}\overset{\searrow}{S} \end{bmatrix} \approx -\frac{\alpha p}{2\beta\rho\frac{\cos j}{\beta}}\left\{a\begin{bmatrix} 1 \\ -1 \end{bmatrix} + d\frac{\cos i}{\alpha}\frac{\cos j}{\beta}\begin{bmatrix} 1 \\ 1 \end{bmatrix}\right\}, \tag{41}$$

$$\begin{bmatrix} \overset{\searrow}{S}\overset{\nearrow}{S} \\ \overset{\searrow}{S}\overset{\searrow}{S} \end{bmatrix} \approx \begin{bmatrix} 0 \\ 1 \end{bmatrix} + \frac{1}{2}\left(\frac{d}{\rho}p^2 - \tan^2 j\frac{\Delta\beta}{\beta}\right)\begin{bmatrix} 1 \\ -1 \end{bmatrix} - \frac{1}{2}\left(\frac{a}{\rho} + \frac{\Delta\beta}{\beta}\right)\begin{bmatrix} 1 \\ 1 \end{bmatrix}, \tag{42}$$

$$\begin{bmatrix} \overset{\searrow}{B}\overset{\nearrow}{S} \\ \overset{\searrow}{B}\overset{\searrow}{S} \end{bmatrix} \approx -\frac{\alpha p}{2\rho\cos i\cos j}\left\{a\cdot\gamma\frac{\cos i}{\alpha}\begin{bmatrix} 1 \\ -1 \end{bmatrix} + d\frac{\cos i}{\alpha}\frac{\cos j}{\beta}\begin{bmatrix} 1 \\ 1 \end{bmatrix}\right\}, \tag{43}$$

$$\begin{bmatrix} \overset{\searrow}{P}\overset{\nearrow}{P} \\ \overset{\searrow}{P}\overset{\searrow}{P} \end{bmatrix} \approx \begin{bmatrix} 0 \\ 1 \end{bmatrix} + \frac{1}{2}\left(\tan^2 i\frac{\Delta\alpha}{\alpha} - \frac{d}{\rho}p^2\right)\begin{bmatrix} 1 \\ 1 \end{bmatrix} + \frac{1}{2}\left[\frac{\Delta\rho}{\rho} + \frac{\Delta\alpha}{\alpha} - \frac{d}{\rho}p^2 - \frac{\gamma^2}{\alpha^2}\frac{\overline{\alpha}^2\overline{M}}{\overline{\alpha}^2\overline{M}-\rho\alpha^2}\left(-\frac{a}{\rho} + \overline{Z}\right) \times\right]\begin{bmatrix} 1 \\ -1 \end{bmatrix}, \tag{44}$$

$$\begin{bmatrix} \overset{\searrow}{S}\overset{\nearrow}{P} \\ \overset{\searrow}{S}\overset{\searrow}{P} \end{bmatrix} \approx -\frac{\beta p}{2\rho\cos i}\left\{a\begin{bmatrix} 1 \\ 1 \end{bmatrix} + \left(1 + \frac{\gamma^2}{\alpha^2}\cdot\frac{\overline{\alpha}^2\overline{M}}{\overline{\alpha}^2\overline{M}-\rho\alpha^2}\right)d\frac{\cos i}{\alpha}\frac{\cos j}{\beta}\begin{bmatrix} 1 \\ -1 \end{bmatrix}\right\}, \tag{45}$$

$$\begin{bmatrix} \overset{\searrow}{B}\overset{\nearrow}{P} \\ \overset{\searrow}{B}\overset{\searrow}{P} \end{bmatrix} \approx -\frac{1}{2\cos i}\left\{\overline{Z} - \frac{a}{\rho}\right\}\begin{bmatrix} 1 \\ 1 \end{bmatrix} + \frac{\gamma}{2\alpha}\left\{\overline{Z} - \frac{d}{\rho}p^2 - \frac{\Delta\overline{M}}{\overline{M}} + 2\frac{\Delta\gamma}{\gamma} + \frac{\overline{\alpha}}{\overline{\alpha}+\delta^B}\left(-\overline{Z} + \frac{\Delta\rho}{\rho} - \frac{\Delta\overline{\alpha}}{\overline{\alpha}}\right)\right\}\begin{bmatrix} 1 \\ -1 \end{bmatrix}. \tag{46}$$

The approximate expressions of scattering coefficients in Eqs. (38)–(46) can be uniformly written as,

$$R'(\theta) \approx a'(\theta)\frac{\Delta\alpha}{\alpha} + b'(\theta)\frac{\Delta\beta}{\beta} + c'(\theta)\frac{\Delta\rho}{\rho} + d'(\theta)\frac{\Delta\gamma}{\gamma} + e'(\theta)\frac{\Delta\overline{\alpha}}{\overline{\alpha}} + f'(\theta)\frac{\Delta\overline{M}}{\overline{M}}. \tag{47}$$

The linear approximation of the scattering coefficient in Eq. (47) includes reflection terms of the fast P-wave velocity $\frac{\Delta\alpha}{\alpha}$, SV-wave velocity $\frac{\Delta\beta}{\beta}$, equivalent density $\frac{\Delta\rho}{\rho}$, slow P-wave velocity $\frac{\Delta\gamma}{\gamma}$, and Biot's parameters $\frac{\Delta\overline{\alpha}}{\overline{\alpha}}$ and $\frac{\Delta\overline{M}}{\overline{M}}$. Its first three terms are similar to Aki and Richards (1980), and last three terms are related to pore and pore fluids, which is an extension of Aki and Richards (1980). As the slow P-wave velocity γ, Biot's parameters $\overline{\alpha}$ and $\overline{M}$ directly reflect the properties of pore and pore fluids (Biot, 1962), realizing high-precision inversion of these parameters can improve the identification accuracy of pore fluids in complex oil and gas reservoirs.

5. Model test and analysis

5.1. Porous media models

For verifying the correctness of the exact analytical expressions 19–27 and the approximate analytical expressions 38–46, and analyzing the effects of pore and pore fluids on response characteristics of elastic wave, a porous media model is established in this paper. In the model, the upper layer is sandstone porous medium with porosity of 0.26 and saturated with oil, and the lower layer is sandstone porous medium with porosity of 0.2 and saturated with brine. Here, the bulk modulus K_s, shear modulus μ_s, and density ρ_s of sandstone matrix are 38GPa, 44GPa, and 2650kg/m^3 (Ren et al., 2009), respectively. Sandstone skeleton parameters are shown in Table 3 and pore fluid parameters are shown in Table 4.

Here, K, μ, f are bulk modulus and shear modulus of rock skeleton, and porosity, respectively. κ, c, $\tilde{a}$ represent rock permeability, tortuosity factor, and pore scale factor, respectively. K_f, ρ_f, η denote bulk modulus, density, and viscosity coefficient of pore fluids, respectively.

Table 3
Sandstone skeleton parameters (Ren et al., 2009).

Model	K(GPa)	μ(GPa)	f	κ(darcy)	$\tilde{c}_m$	$\tilde{a}$(m)
Upper layer	7.49	5.67	0.26	1.6	1.72	10^{-6}
Lower layer	16.9	13.96	0.20	0.2	1.62	10^{-6}

Table 4
Pore fluid parameters (Zhao et al., 2015).

Model	Gas	Oil	Brine
K_f(GPa)	0.012	2.1	3.0
ρ_f(kg/m^3)	78.0	940	1050
η(cP)	0.15	5.0	1.6

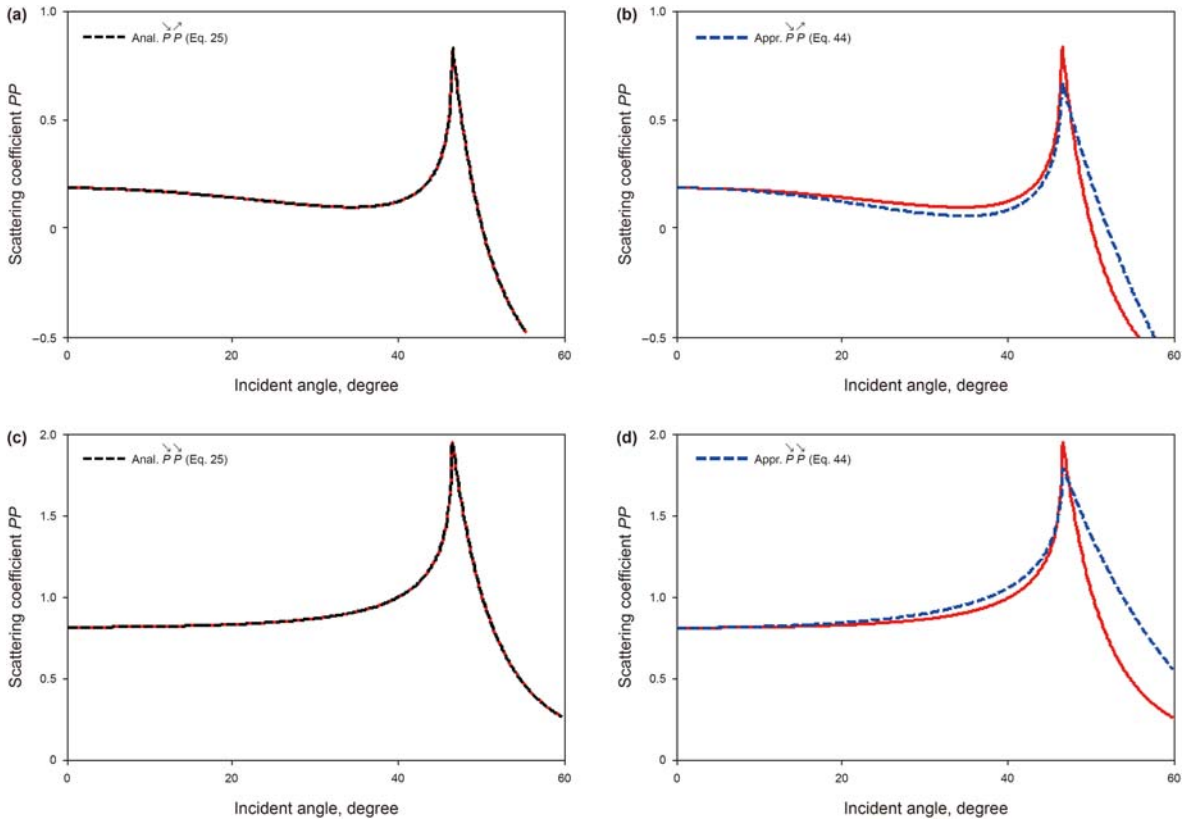

Fig. 3. Scattering coefficients of the fast P-wave with the fast P-wave being incident.
Figures (a) and (b) are reflection coefficients, and (c) and (d) represent transmission coefficients of the fast P-wave. The red solid line, black and blue dotted lines denote scattering coefficients of exact equation (Eq. (16)), exact analytical expressions (Eq. (25)), and first-order linear approximations (Eq. (44)), respectively.

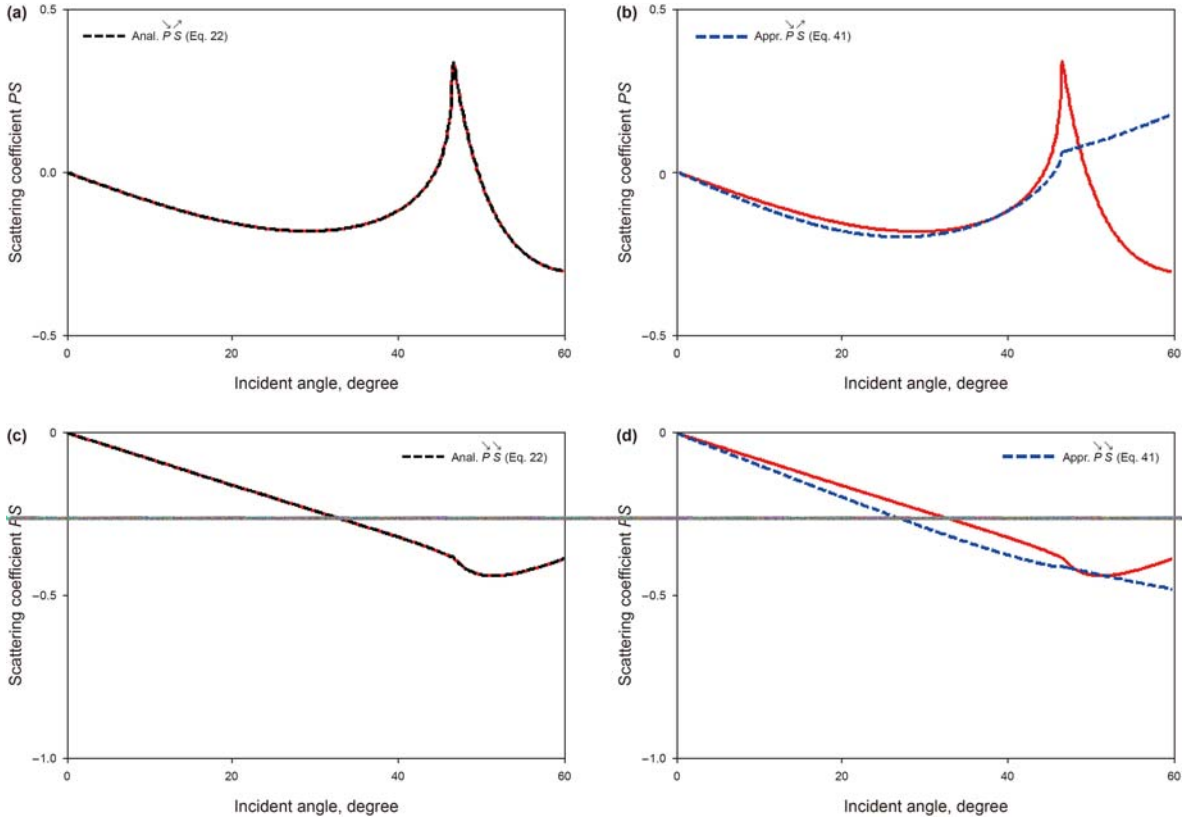

Fig. 4. Scattering coefficients of the SV-wave with the fast P-wave being incident.
The meanings of the subgraphs are similar to that in Fig. 3. The black and blue dotted lines represent scattering coefficients calculated by exact analytical expression (Eq. (22)) and first-order linear approximation (Eq. (41)), respectively.

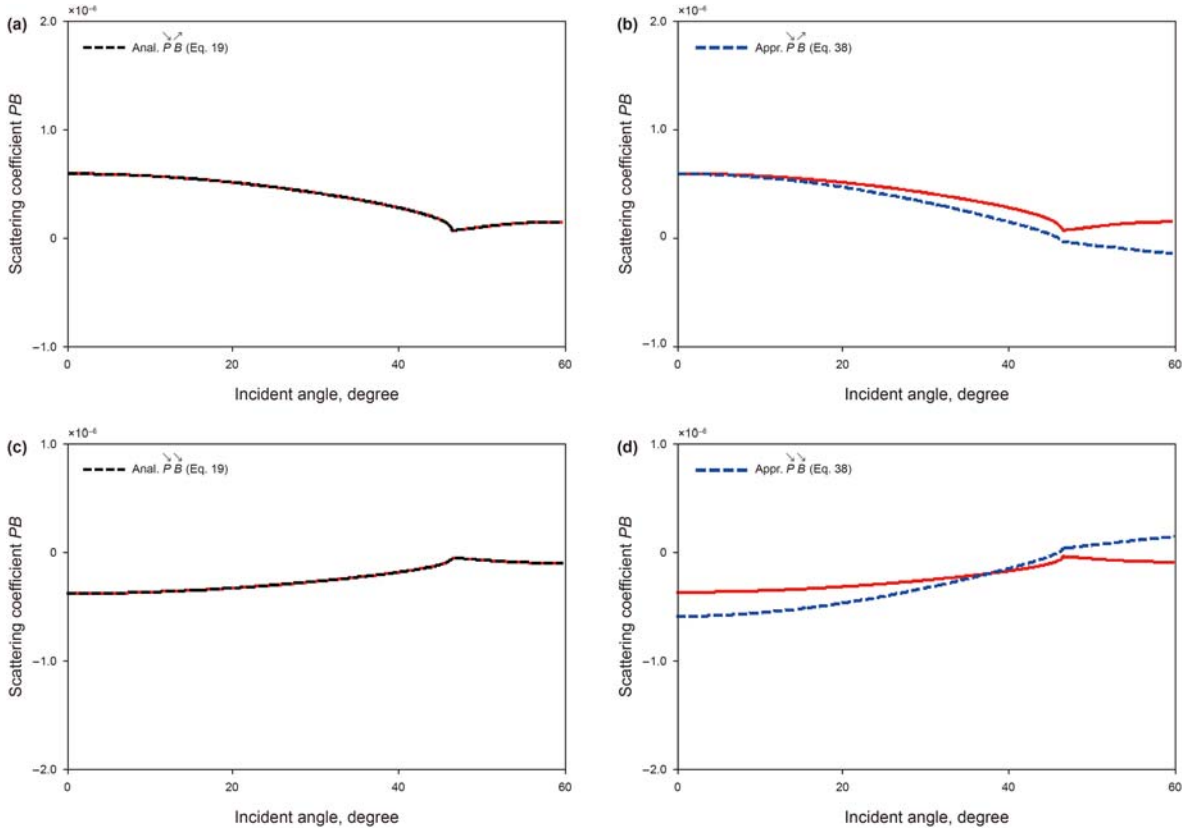

Fig. 5. Scattering coefficients of the slow P-wave with the fast P-wave being incident.
The meanings of the subgraphs are similar to that in Fig. 3. The black and blue dotted lines represent scattering coefficients calculated by exact analytical expression (Eq. (19)) and first-order linear approximation (Eq. (38)), respectively.

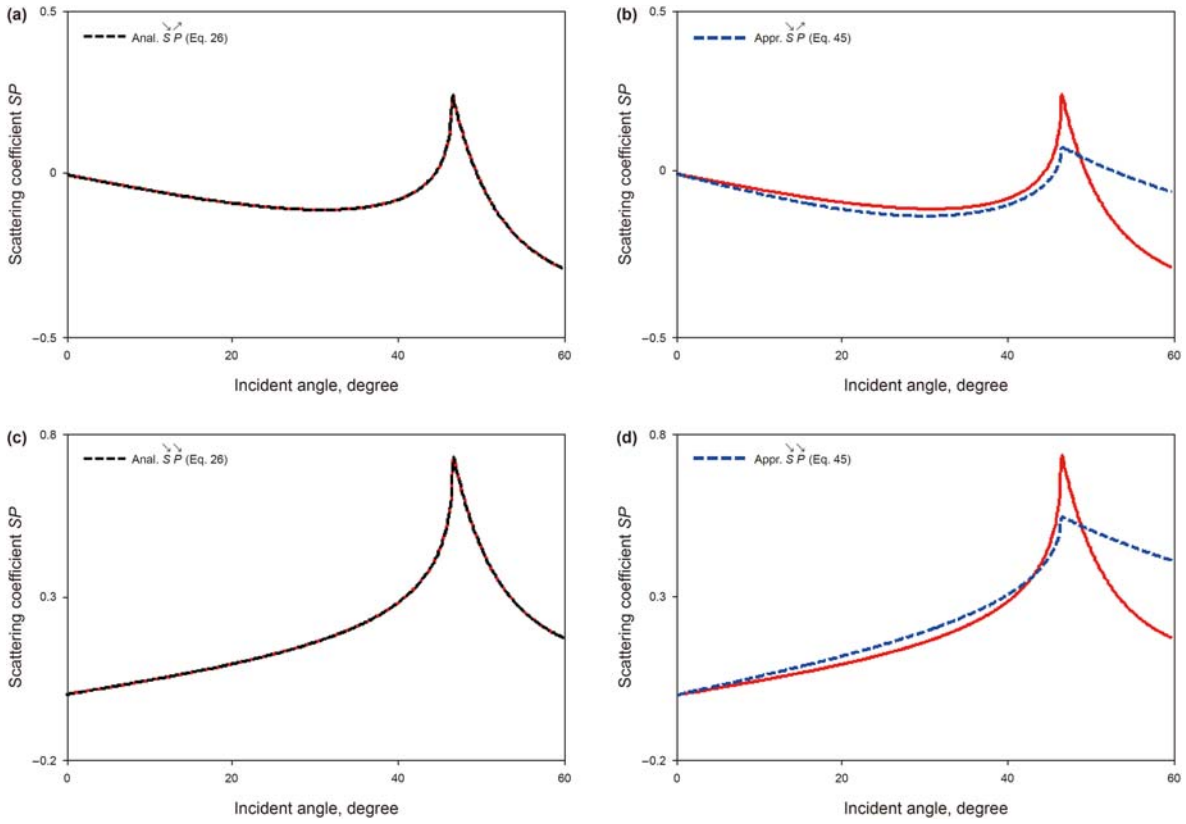

Fig. 6. Scattering coefficients of the fast P-wave with the SV-wave being incident.
The meanings of the subgraphs are similar to that in Fig. 3. The black and blue dotted lines represent scattering coefficients calculated by exact analytical expression (Eq. (26)) and first-order linear approximation (Eq. (45)), respectively.

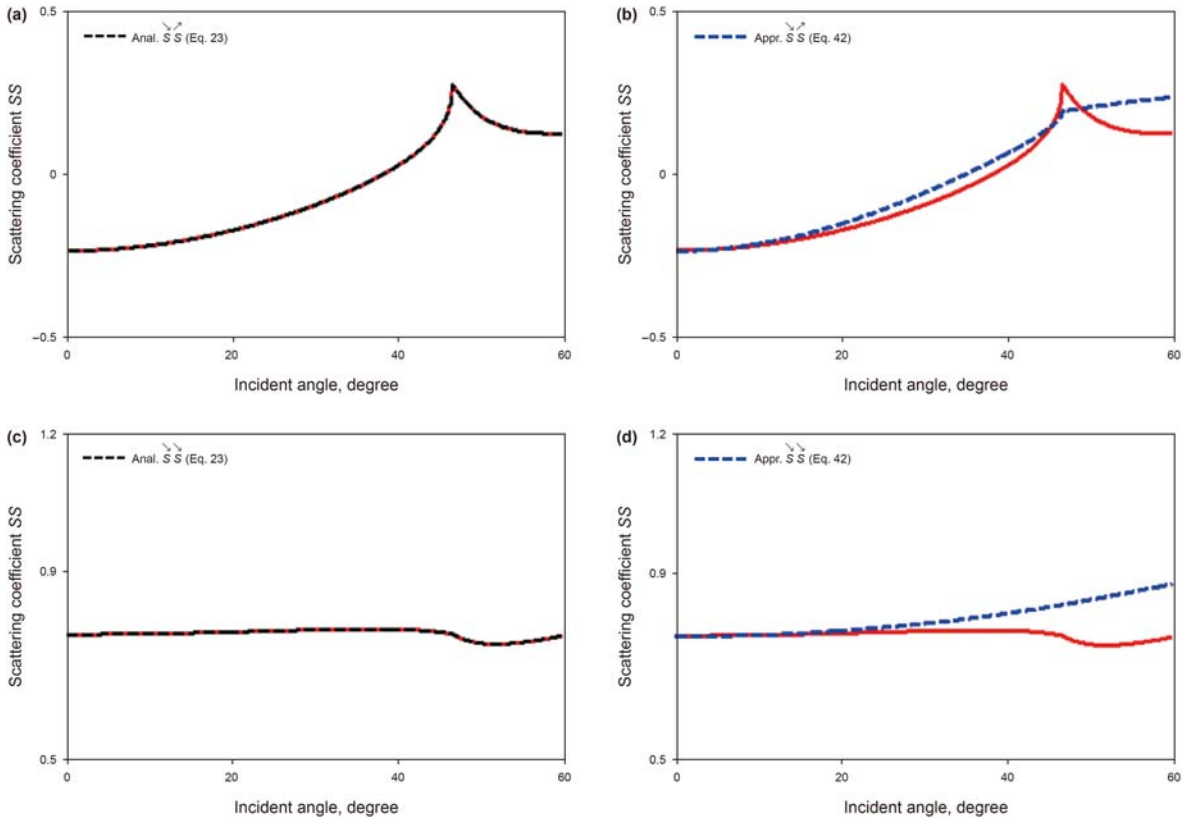

Fig. 7. Scattering coefficients of the SV-wave with the SV-wave being incident.
The meanings of the subgraphs are similar to that in Fig. 3. The black and blue dotted lines represent scattering coefficients calculated by exact analytical expression (Eq. (23)) and first-order linear approximation (Eq. (42)), respectively.

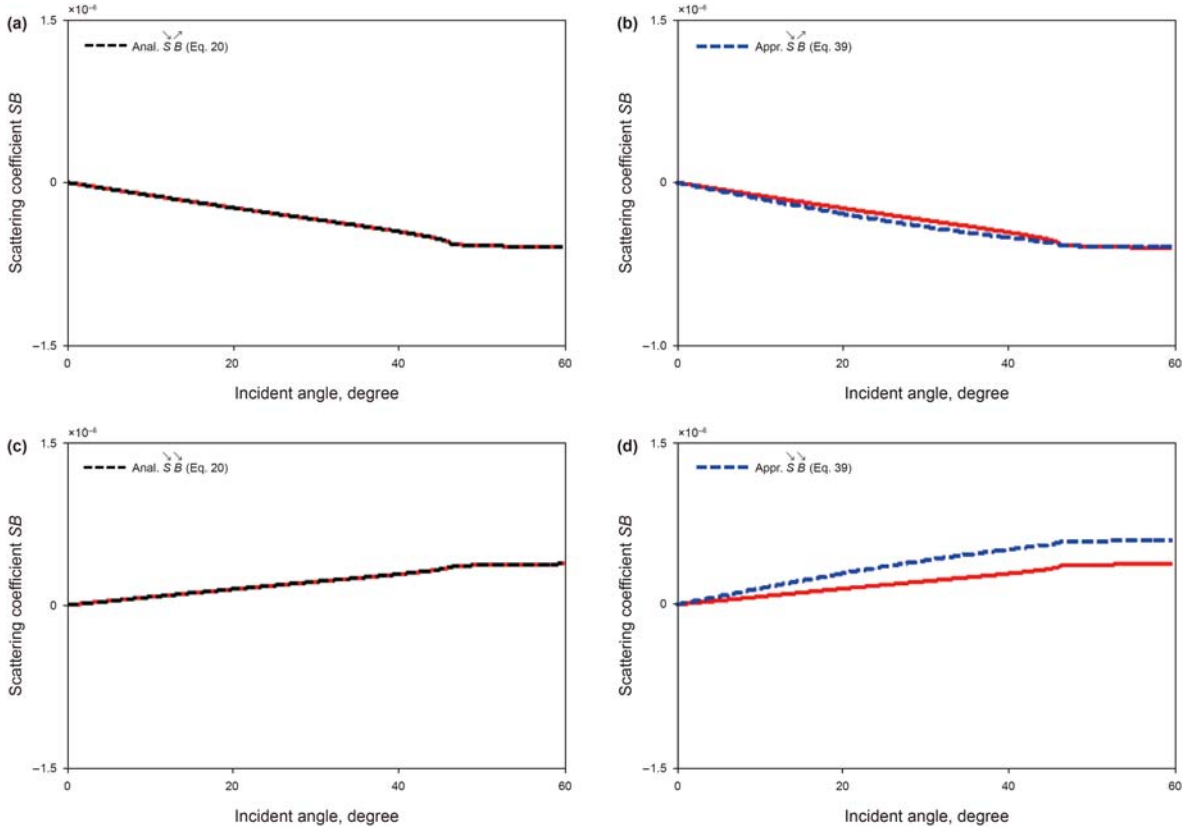

Fig. 8. Scattering coefficients of the slow P-wave with the SV-wave being incident.
The meanings of the subgraphs are similar to that in Fig. 3. The black and blue dotted lines represent scattering coefficients calculated by exact analytical expression (Eq. (20)) and first-order linear approximation (Eq. (39)), respectively.

5.2. Scattering coefficients corresponding to the incident fast P-wave

Substituting the parameters of lithology and pore fluids in Tables 3 and 4 into the analytical equation (Eq. (16)), exact analytical expressions (Eqs. (19)–(27)), and first-order linear approximations (Eqs. (28)–(36)), we verify the correctness of the derived analytical equations and expressions, and analyze the response characteristics of various scattered waves. Fig. 3 shows scattering coefficients with the fast P-wave being incident. Wherein, subgraphs (a) and (b) represent the reflection coefficients of the fast P-wave, and (c) and (d) denote the transmission coefficients of the fast P-wave. The red solid line, the black and blue dotted lines represent the scattering coefficients calculated by the exact equations (Eq. (16)), the exact analytical expressions (Eq. (25)), and the first-order linear approximation (Eq. (44)), respectively. Figs. 4 and 5 show the scattering coefficients of the SV- and slow P-waves with the fast P-wave being incident, respectively, and the meaning of their subgraphs is similar to that in Fig. 3. The black and blue dotted lines in Fig. 4 are calculated by Eqs. (22) and (41), respectively, and that in Fig. 5 are calculated by Eqs. (19) and (38), respectively.

According to the analysis of Figs. 3-5,

1) The scattering coefficients (black dotted line) calculated by exact analytical expressions (Eqs. (25), (22), and (19)) are consistent with that (red solid lines) calculated by exact equation (Eq. (16)) in Fig. 3a and c, which shows that our deduced exact analytical expressions are correct, and the same conclusion can be obtained by analyzing subgraphs (a) and (c) in Figs. 4 and 5.
2) The scattering coefficients (blue dotted line) calculated by first-order approximate analytical expressions (Eqs. (44), (41), and (38)) have a similar variation curve with that (red solid line) calculated by exact equation (Eq. (16)), which shows the correctness of our derived approximate analytical expressions to a certain extent.
3) Depending on the influence degree of truncation error (ignoring second- and higher order terms), the critical angles of scattering coefficient of the SV-wave first-order approximation (Eq. (41), and Fig. 4b and d) are smaller than that of fast P-wave (Eq. (44), and Fig. 3b and d). The scattering coefficients of the slow P-wave are small, and their first-order approximations are greatly affected by the truncation error (Fig. 5b and d).

5.3. Scattering coefficients corresponding to the incident SV-wave

Figs. 6–8 show scattering coefficients of the fast P-, SV-, and slow P-waves, respectively, and the meanings of their subgraph are similar to that in Fig. 3. In Figs. 6–8, black dotted lines represent scattering coefficients calculated by exact analytical expressions (Eqs. (26), (23), and (20), respectively), and blue dotted lines are that calculated by first-order approximations (Eqs. (45), (42), and (39), respectively).

According to Figs. 6–8.

1) When the incident angle is less than 40°, scattering coefficients (blue dotted lines) calculated by first-order linear approximations (Eqs. (45), (42), and (39)) in Figs. 6b–8b and 6d-8d are basically consistent with that (red solid lines) calculated by exact equation (Eq. (16)), which shows that the deduced first-order linear approximations with the SV-wave being incident are correct.

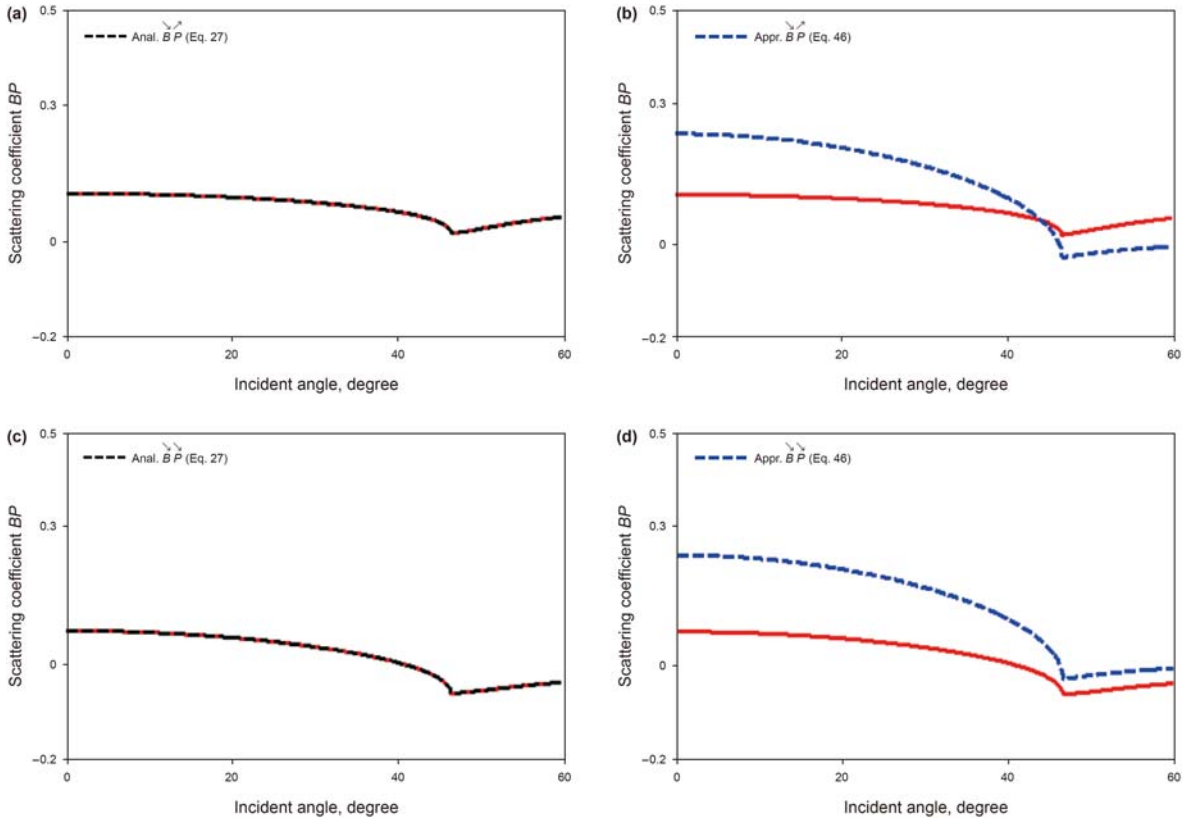

Fig. 9. Scattering coefficients of the fast P-wave with the slow P-wave being incident.
The meanings of the subgraphs are similar to that in Fig. 3. The black and blue dotted lines represent scattering coefficients calculated by exact analytical expression (Eq. (27)) and first-order linear approximation (Eq. (46)), respectively.

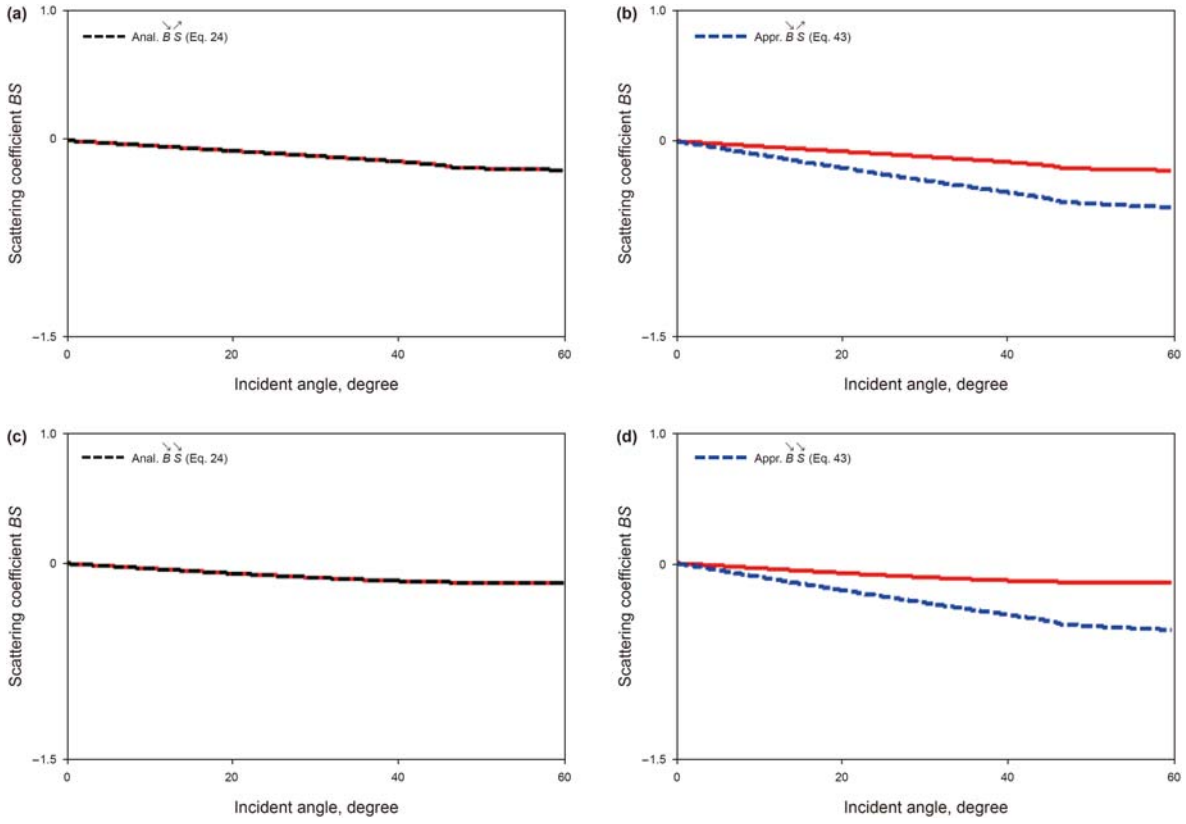

Fig. 10. Scattering coefficient of the SV-wave with the slow P-wave being incident.
The meanings of the subgraphs are similar to that in Fig. 3. The black and blue dotted lines represent scattering coefficients calculated by exact analytical expression (Eq. (24)) and first-order linear approximation (Eq. (43)), respectively.

2) However, as different contribution of each-order term to different approximate expressions, the accuracy of different first-order approximations is also different. The fast P-wave's accuracy is higher (Fig. 6b and d), and the SV-wave's accuracy is relatively lower (Fig. 7b and d).
3) As scattering coefficients of the slow P-wave are very small, and are greatly affected by the weak elastic assumption and the neglect of second- and higher-order terms, the accuracy of approximate expressions of the slow P-wave with the SV-wave being incident is relatively low (Fig. 8b and d).

5.4. Scattering coefficients corresponding to the incident slow P-wave

Except for the case of the fast P- and SV-waves being incident, the characteristics of scattering coefficient of the slow P-wave being incident are further analyzed in this paper. Figs. 9–11 respectively show the scattering coefficients of the fast P-, SV- and slow P-waves with the slow P-wave being incident, and the meanings of their subgraphs are similar to that in Fig. 3. In Figs. 9–11, the black dotted lines represent scattering coefficients calculated by accurate analytical expressions (Eqs. (27), (24) and (21), respectively), and the blue dotted lines are that calculated by first-order linear approximate expressions (Eqs. (46), (43), and (40), respectively).

From Figs. 9–11,

1) In the case of the slow P-wave incidence, the scattering coefficients calculated by first-order approximations of the fast P-, SV-, and slow P-waves (Eqs. (46), (43), and (40)) are basically the same as that calculated by analytical equation (Eq. (16)). However, the accuracy of approximate expressions (Eqs. (46), (43), and (40)) are relatively low due to the limitations of small angle incidence, weak elasticity at a porous media interface, and ignoring the second- and higher-order terms.
2) For the incident and scattering system of P-SV-B plane waves (Fig. 1), under the assumption that various elastic waves and corresponding incident angles meet Snell's law (Eq. (13)), the incidence or scattering of the slow P-wave is very weakly dependent on incident angle of the fast P-wave. Analyzing approximate expression (Eq. A-6), approximate equation (Eq. (17)), and accurate analytical expression (Eq. (21)), the expression of $\left(\frac{\gamma}{\alpha}\right)^2 \cdot \frac{d\rho^2}{\rho} = 2\left(\frac{\beta}{\alpha}\right)^2 \left(2\frac{\Delta\beta}{\beta} + \frac{\Delta\rho}{\rho}\right)\sin^2 k$ in Eq. (40) tends to zero, which show that the scattering coefficients of the slow P-wave with the slow P-wave being incident do not depend on incident angle of the fast P-wave (Fig. 11b and d).
3) As the fast P- and SV-waves depend on incident angle of the fast P-wave, the scattering coefficients of converted waves related to the slow P-wave are weakly dependent on the angle, e.g. the slow P-wave scattering coefficients with the fast P-wave being incident in Eq. (38) (Fig. 5b and d).

6. Conclusions

Pre-stack AVO inversion plays an important role in reservoir prediction and fluid identification, and its theoretical basis is Zoeppritz and Aki and Richards approximation. However, for complex oil and gas reservoirs, the theoretical basis has certain application limitations. As reservoir rock containing pores, the

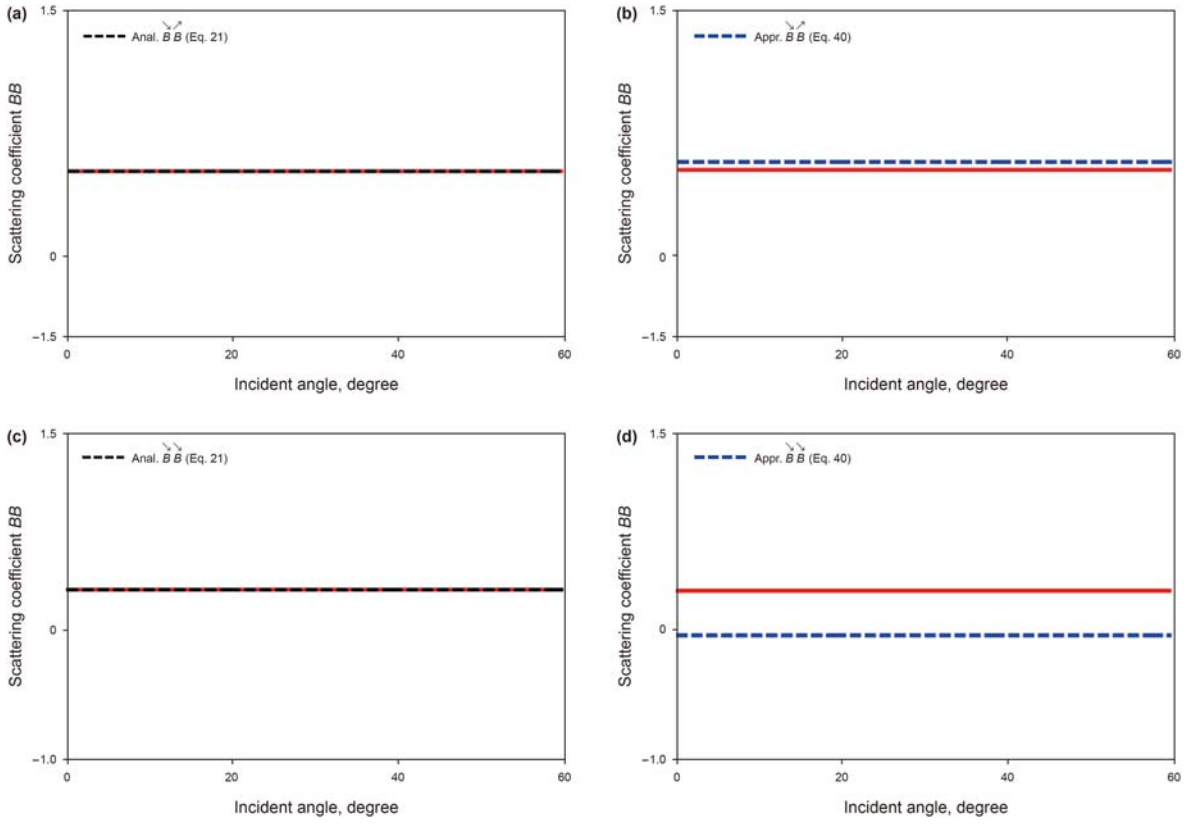

Fig. 11. Scattering coefficient of the slow P-wave with the slow P-wave being incident.
The meanings of the subgraphs are similar to that in Fig. 3. The black and blue dotted lines represent scattering coefficients calculated by exact analytical expression (Eq. (21)) and first-order linear approximation (Eq. (40)), respectively.

influence of rock pore's size, shape, diameter, and its filler on elastic wave's response can not be ignored. Further study on the influence of these factors is great significance to further solve the prediction of complex oil and gas reservoirs and to improve the accuracy of reservoir fluid identification. Based on previous achievements, this paper studies the approximate scattering of elastic plane wave at an interface of porous media saturated with pore fluids. Firstly, the incidence, reflection and transmission at an interface of porous media are analyzed, and a complete system of incidence and scattering of P-SV-B waves is established. Secondly, the kinematic and dynamic boundary conditions at an interface of porous media are constructed. Finally, exact analytical equation and expressions of elastic plane wave for porous media are derived, respectively, and the first-order linear approximate expressions are obtained under various priori assumptions.

Unlike Zoeppritz equation and its approximate expressions, which only considers the reflection and transmission characteristics at the interface of single-phase media, the kinematic and dynamic characteristics of rock skeleton and pore fluids are considered at the porous media interface. However, the case of porous media is much more complex than that of single-phase medium, and the derivation of the analytical equations or expressions need to be based on a series of assumptions. Assumptions for the derivation of analytical equation are: 1) The upper and lower porous media are isotropic and uniform media; 2) The porous media interface is a horizontal interface, and the upper and lower rock skeletons are seamless contact; 3) The pores are completely connected, and pore fluids are Newtonian fluids; 4) Pore fluid is non-viscous fluid, and the interaction between rock skeleton and pore fluid is not considered; 5) The fast P-, SV-, and slow P-waves propagating in upper and lower porous media meet Snell's law. Assumptions for the derivations of first-order approximate expressions are: 1) Various incident waves are incident with small angles (usually below 40°); 2) The difference of elastic parameters between upper and lower layers is small, that is, there is a weak elastic hypothesis at an interface of porous media; 3) The constant and first-order terms are retained, and others are ignored; 4) The frequency of incident wave is in the range of seismic frequency, and the slow P-wave is close to vertical incidence and scattering.

Combined with our research results, the inversion of pore fluid parameters based on porous media theory can be realized. Realizing these parameters inversion can further solve the problem of low identification accuracy of pore fluids in complex oil and gas reservoirs. However, our research results are derived on the basis of a series of assumptions, and there may still be some application limitations for more complex reservoirs. This requires following researchers to further consider the more complex situations of porous media. For example, the upper and lower rock skeletons are sliding, pores are not completely connected, pore fluids are viscous, and are coupled with rock skeleton, etc. The research on analytical theory of elastic plane wave for these complex porous media will provide theoretical support for further solving the problems of oil and gas identification, and improving the accuracy of oil and gas exploration and development.

Acknowledgements

This study was financially supported by the National Natural Science Foundation of China (Grant No. 42104131), the Natural Science Foundation of Sichuan Province of China (Grant No. 2022NSFSC1140), Open Fund (PLC20211101) of State Key Laboratory of Oil and Gas Reservoir Geology and Exploitation. Data is available

through Ren et al. (2009) [https://doi.org/10.1190/1.3207863] and Zhao et al. (2015) [https://doi.org/10.1190/geo2014-0307.1]. The authors are also grateful to the anonymous reviewers for their constructive comments.

Appendix A. Simplification and Approximation for Exact Analytic Equation

The following relationships between the P- and SV-wave velocities, density, bulk and shear moduli, and Biot's parameters can be obtained (Russell et al., 2011).

$$\rho\alpha^2 = K + \overline{\alpha}^2\overline{M} + \frac{4}{3}\mu \tag{A-1a}$$

$$\rho\beta^2 = \mu \tag{A-1b}$$

$$\rho = (1-\varphi')\rho_b + \varphi'\rho_f = \rho_b + \varphi'\left(\rho_f - \rho_b\right) \tag{A-2}$$

where, ρ, ρ_b, ρ_f denote the total density, rock matrix density, and pore fluid density, respectively, and φ' is porosity.

Following the papers of Biot (1962), Russell et al. (2003), Dai et al. (2006), and Zhou et al. (2020), within the seismic frequency band, the ratios between displacement amplitude of pore fluid relative to rock skeleton and that of rock skeleton generated by the fast P-, SV- and slow P-waves can be approximately,

$$\delta^P = \frac{K + \frac{4}{3}\mu + \overline{\alpha}^2\overline{M} - \rho_b\alpha^2}{-\overline{\alpha}\overline{M} + \rho_f\alpha^2} \approx 0 \tag{A-3a}$$

$$\delta^{SV} = \frac{\mu - \rho_b\beta^2}{\rho_f\beta^2} \approx 0 \tag{A-3b}$$

$$\delta^B = \frac{K + \frac{4}{3}\mu + \overline{\alpha}^2\overline{M} - \rho_b\gamma^2}{-\overline{\alpha}\overline{M} + \rho_f\gamma^2} \approx -\frac{\rho\alpha^2}{\overline{\alpha}\overline{M}} \tag{A-3c}$$

Equations A-3 shows that compared with the displacement of rock skeleton caused by the fast P-wave, the displacement of pore fluids relative to rock skeleton can be ignored, while that caused by slow P-wave can not be ignored. Without considering the viscosity of pore fluids, the SV-wave can not cause the relative displacement between pore fluids and rock skeleton.

Substituting Eqs. A-1~A-3 into the relevant parameter group in the coefficient matrix of Eq. (15), the following approximate expressions are obtained,

$$\frac{1}{\alpha}\left[\left(K + \overline{\alpha}^2\overline{M} + \delta^P\overline{\alpha}\overline{M} - \frac{2}{3}\mu\right) + 2\mu\left(1 - \alpha^2p^2\right)\right] \approx \rho\alpha\left(1 - 2\beta^2p^2\right) \tag{A-4a}$$

$$\frac{1}{\gamma}\left[\left(K + \overline{\alpha}^2\overline{M} - \frac{2}{3}\mu + \delta^B\overline{\alpha}\overline{M}\right) + 2\mu\left(1 - \gamma^2p^2\right)\right] \approx \rho\gamma\left(1 - 2\beta^2p^2\right) \tag{A-4b}$$

$$\frac{(\overline{\alpha} + \delta^P)\overline{M}}{\alpha} \approx \frac{\overline{\alpha}\overline{M}}{\alpha} \tag{A-5}$$

When the incident wave frequency is within the seismic frequency band, the relationship among the velocities of the fast P-, SV-, and slow P-waves is $\gamma \ll \beta < \alpha$. By substituting this into Eq. (13), the following approximate equation can be obtained,

$$\begin{aligned} &k \ll j < i, \ \sin k = \frac{\gamma}{\alpha}\sin i \to 0 \\ &\cos k \approx 1 \end{aligned} \tag{A-6}$$

Appendix B. Solving Approximate Analytical Equation

For solving the approximate analytic Eq. (17c), it is necessary to first solve the inverse problem of the two-dimensional (2D) and three-dimensional (3D) block matrices. Equations B-1 and B-2 (Lu, 2010) can be used to obtain the 2D and 3D block inverse matrices, respectively.

$$\begin{bmatrix} A & B \\ C & D \end{bmatrix}^{-1} = \begin{bmatrix} C^{-1}\left(AC^{-1} - BD^{-1}\right)^{-1} & A^{-1}\left(CA^{-1} - DB^{-1}\right)^{-1} \\ -D^{-1}\left(AC^{-1} - BD^{-1}\right)^{-1} & -B^{-1}\left(CA^{-1} - DB^{-1}\right)^{-1} \end{bmatrix} \tag{B-1}$$

$$\begin{bmatrix} A & B & C \\ D & E & F \\ G & H & K \end{bmatrix}^{-1} = \begin{bmatrix} A^{-1} + PT^{-1}Q & PT^{-1} \\ T^{-1}Q & T^{-1} \end{bmatrix} \tag{B-2}$$

$$P = \begin{bmatrix} -A^{-1}B & -A^{-1}C \end{bmatrix},$$

Here, $Q = \begin{bmatrix} -DA^{-1} \\ -GA^{-1} \end{bmatrix}$,

$$T = \begin{bmatrix} E - DA^{-1}B & F - DA^{-1}C \\ H - GA^{-1}B & K - GA^{-1}C \end{bmatrix}.$$

From Eq. B-2, we know that obtaining the inverse matrix of T is the key to solving the 3D inverse block matrix. As submatrix of T is a 2D block matrix, by substituting the elements in matrix T into Eq. B-1, and fully considering submatrix of $H = \begin{bmatrix} 0 & 0 \\ 0 & 0 \end{bmatrix}$, we can deduce,

$$T^{-1} = \begin{bmatrix} S_{11}V_2D^{-1} & -S_{11} \\ S_{21}V_1D^{-1} & S_{21} \end{bmatrix} \tag{B-3}$$

$$S_{11} = \left(D^{-1}E - A^{-1}B\right)^{-1}(V_1 + V_2)^{-1} \tag{B-4a}$$

$$S_{21} = \left(D^{-1}F - A^{-1}C\right)^{-1}(V_1 + V_2)^{-1} \tag{B-4b}$$

$$V_1 = GA^{-1}B \cdot \left(D^{-1}E - A^{-1}B\right)^{-1} \tag{B-5a}$$

$$V_2 = \left(K - GA^{-1}C\right)\left(D^{-1}F - A^{-1}C\right)^{-1} \tag{B-5b}$$

Substituting Eq. B-3 into Eq. B-2, the 3D inverse block matrix (Eq. B-2) is finally derived as,

$$\begin{bmatrix} A & B & C \\ D & E & F \\ G & H & K \end{bmatrix}^{-1} = \begin{bmatrix} A^{-1} + A^{-1}\begin{bmatrix} BS_{11}(V_2 - G) \\ +CS_{21}(V_1 + G) \end{bmatrix}A^{-1} & -A^{-1}(BS_{11}V_2 + CS_{21}V_1)D^{-1} & A^{-1}(BS_{11} - CS_{21}) \\ -S_{11}(V_2 - G)A^{-1} & S_{11}V_2D^{-1} & -S_{11} \\ -S_{21}(V_1 + G)A^{-1} & S_{21}V_1D^{-1} & S_{21} \end{bmatrix} \tag{B-6}$$

Substituting Eq. B-6 into Eq. (17c), the following expression can be obtained,

$$\begin{bmatrix} \langle 1\rangle & \langle 2\rangle & \langle 3\rangle \\ \langle 4\rangle & \langle 5\rangle & \langle 6\rangle \\ \langle 7\rangle & \langle 8\rangle & \langle 9\rangle \end{bmatrix} = \begin{bmatrix} A^{-1}+A^{-1}[BS_{11}(V_2-G)+CS_{21}(V_1+G)]A^{-1} & -A^{-1}(BS_{11}V_2+CS_{21}V_1)D^{-1} & A^{-1}(BS_{11}-CS_{21}) \\ -S_{11}(V_2-G)A^{-1} & S_{11}V_2D^{-1} & -S_{11} \\ -S_{21}(V_1+G)A^{-1} & S_{21}V_1D^{-1} & S_{21} \end{bmatrix} \cdot \begin{bmatrix} -A & -B & -C \\ D & E & F \\ -G & 0 & K' \end{bmatrix} \tag{B-7}$$

Solving Eq. B-7, and fully considering relationships among 2D submatrices A ~ K (Eq. B-8), the expressions of submatrices $\langle 1\rangle \sim \langle 9\rangle$ can be derived as in Eq. B-9.

$$\left(D^{-1}E-A^{-1}B\right)S_{11}=\left(D^{-1}F-A^{-1}C\right)S_{21} \tag{B-8a}$$

$$D^{-1}(ES_{11}-FS_{21})=A^{-1}(BS_{11}-CS_{21}) \tag{B-8b}$$

$$D^{-1}ES_{11}+A^{-1}CS_{21}=A^{-1}BS_{11}+D^{-1}FS_{21} \tag{B-8c}$$

$$\begin{bmatrix} \langle 1\rangle & \langle 2\rangle & \langle 3\rangle \\ \langle 4\rangle & \langle 5\rangle & \langle 6\rangle \\ \langle 7\rangle & \langle 8\rangle & \langle 9\rangle \end{bmatrix} = \begin{bmatrix} -\left\{I+A^{-1}B\cdot\langle 4\rangle+A^{-1}C\cdot\langle 7\rangle\right\} & -\left\{A^{-1}B(I+\langle 5\rangle)+A^{-1}C\cdot\langle 8\rangle\right\} & -\left\{A^{-1}B\cdot\langle 6\rangle+A^{-1}C\cdot(I+\langle 9\rangle)\right\} \\ 2S_{11}V_2 & \frac{1}{2}\cdot\langle 4\rangle\cdot\left(A^{-1}B+D^{-1}E\right)-S_{11}GA^{-1}B & \langle 4\rangle\cdot D^{-1}F-S_{11}K'' \\ 2S_{21}V_1 & \langle 7\rangle\cdot D^{-1}E & \frac{1}{2}\cdot\langle 7\rangle\cdot\left(A^{-1}C+D^{-1}F\right)+S_{21}\left(GA^{-1}C+K'\right) \end{bmatrix} \tag{B-9}$$

Appendix C. Analytical Solutions of Submatrix and Its Composite Forms

For obtaining the complete analytical expressions of scattering coefficients (Eqs. (19)–(27)), only the nine submatrices in Eq. (18) need to be solved independently. In the process of substituting lithology parameters and pore fluid parameters of upper and lower media into Eq. (18), the solution operation of the submatrices and their composite expressions will be involved. The relevant analytical expressions are,

$$A^{-1}=\frac{1}{-\alpha_1\alpha_2 p\cdot a}\begin{bmatrix} \rho_2\alpha_2\left(1-2\beta_2^2p^2\right) & -\alpha_2 p \\ \rho_1\alpha_1\left(1-2\beta_1^2p^2\right) & -\alpha_1 p \end{bmatrix}, \tag{C-1a}$$

$$D^{-1}=\frac{1}{\cos i_1\cos i_2\cdot p\cdot d}\begin{bmatrix} 2\rho_2\beta_2^2 p\cos i_2 & -\cos i_2 \\ -2\rho_1\beta_1^2 p\cos i_1 & \cos i_1 \end{bmatrix} \tag{C-1b}$$

$$A^{-1}B=\frac{1}{-\alpha_1\alpha_2 p\cdot a}\begin{bmatrix} -\alpha_2\cdot b\cdot\cos j_1 & \alpha_2\cdot\rho_2\cdot\cos j_2 \\ -\alpha_1\cdot\rho_1\cdot\cos j_1 & \alpha_1\cdot c\cdot\cos j_2 \end{bmatrix} \tag{C-1c}$$

$$A^{-1}C=\begin{bmatrix} \gamma_1/\alpha_1 & 0 \\ 0 & \gamma_2/\alpha_2 \end{bmatrix}, \tag{C-1d}$$

$$GA^{-1}B=\frac{1}{-p\cdot a}\cdot\begin{bmatrix} 0 & 0 \\ (l\cdot\rho_1-s\cdot b)\cos j_1 & -(l\cdot c-s\cdot\rho_2)\cos j_2 \end{bmatrix}, \tag{C-2a}$$

$$GA^{-1}C=\begin{bmatrix} 0 & 0 \\ s\cdot\gamma_1 & -l\cdot\gamma_2 \end{bmatrix} \tag{C-2b}$$

$$D^{-1}E=\frac{1}{\cos i_1\cos i_2\cdot p\cdot d}\begin{bmatrix} -\beta_1\cdot c\cdot\cos i_2 & -\beta_2\cdot\rho_2\cdot\cos i_2 \\ \beta_1\cdot\rho_1\cdot\cos i_1 & \beta_2\cdot b\cdot\cos i_1 \end{bmatrix} \tag{C-2c}$$

$$D^{-1}F=\frac{1}{\cos i_1\cos i_2}\begin{bmatrix} \cos i_2 & 0 \\ 0 & \cos i_1 \end{bmatrix}. \tag{C-2d}$$

$$D^{-1}E-A^{-1}B=\frac{\beta_1\beta_2}{adp\cdot\cos i_1\cos i_2}\begin{bmatrix} -\frac{\alpha_2}{\beta_2}\frac{\cos i_2}{\alpha_2}\cdot\overline{Q} & -\frac{\alpha_2}{\beta_1}\frac{\cos i_2}{\alpha_2}\cdot\rho_2\overline{G} \\ \frac{\alpha_1}{\beta_2}\frac{\cos i_1}{\alpha_1}\cdot\rho_1\overline{H} & \frac{\alpha_1}{\beta_1}\frac{\cos i_1}{\alpha_1}\cdot\overline{R} \end{bmatrix} \tag{C-3a}$$

$$\left(D^{-1}E-A^{-1}B\right)^{-1}=\frac{ap}{\overline{X}}\begin{bmatrix} \frac{\alpha_1}{\beta_1}\frac{\cos i_1}{\alpha_1}\cdot\overline{R} & \frac{\alpha_2}{\beta_1}\frac{\cos i_2}{\alpha_2}\cdot\rho_2\overline{G} \\ -\frac{\alpha_1}{\beta_2}\frac{\cos i_1}{\alpha_1}\cdot\rho_1\overline{H} & -\frac{\alpha_2}{\beta_2}\frac{\cos i_2}{\alpha_2}\cdot\overline{Q} \end{bmatrix} \tag{C-3b}$$

$$A^{-1}B+D^{-1}E=\frac{\beta_1\beta_2}{adp\cdot\cos i_1\cos i_2}\begin{bmatrix} -\frac{\overline{Q}'}{\beta_2}\cos i_2 & -\frac{\rho_2\overline{G}'}{\beta_1}\cos i_2 \\ \frac{\rho_1\overline{H}'}{\beta_2}\cos i_1\cdot & \frac{\overline{R}'}{\beta_1}\cos i_1 \end{bmatrix}. \tag{C-3c}$$

$$D^{-1}F-A^{-1}C=\frac{1}{\alpha_1\alpha_2\cos i_1\cos i_2}\begin{bmatrix} \alpha_2\cdot g\cdot\cos i_2 & 0 \\ 0 & \alpha_1\cdot h\cdot\cos i_1 \end{bmatrix} \tag{C-4a}$$

$$\left(D^{-1}F-A^{-1}C\right)^{-1}=\frac{1}{gh}\begin{bmatrix} \alpha_1 h\cos i_1 & 0 \\ 0 & \alpha_2 g\cos i_2 \end{bmatrix} \tag{C-4b}$$

$$D^{-1}F+A^{-1}C=\frac{1}{\alpha_1\alpha_2\cos i_1\cos i_2}\begin{bmatrix}\alpha_2(\alpha_1+\gamma_1\cos i_1)\cos i_2 & 0\\ 0 & \alpha_1(\alpha_2+\gamma_2\cos i_2)\cos i_1\end{bmatrix}. \tag{C-4c}$$

$$K-GA^{-1}C=\begin{bmatrix}\delta_1^B & \delta_2^B\\ \dfrac{\overline{U}}{\gamma_1} & -\dfrac{\overline{V}}{\gamma_2}\end{bmatrix} \tag{C-5a}$$

$$K'+GA^{-1}C=\begin{bmatrix}\delta_1^B & \delta_2^B\\ -\dfrac{\overline{U}}{\gamma_1} & \dfrac{\overline{V}}{\gamma_2}\end{bmatrix}. \tag{C-5b}$$

$$V_1=-\frac{1}{\tilde{X}}\begin{bmatrix}0 & 0\\ \left(\tilde{R}\dfrac{\cos j_1}{\beta_1}+\tilde{H}\dfrac{\cos j_2}{\beta_2}\right)\cos i_1 & \left(\tilde{G}\dfrac{\cos j_1}{\beta_1}+\tilde{Q}\dfrac{\cos j_2}{\beta_2}\right)\cos i_2\end{bmatrix} \tag{C-6a}$$

$$V_2=\frac{1}{gh}\cdot\begin{bmatrix}\delta_1^B\cdot\alpha_1\cdot h\cdot\cos i_1 & \delta_2^B\cdot\alpha_2\cdot g\cdot\cos i_2\\ \dfrac{\overline{U}}{\gamma_1}\cdot\alpha_1\cdot h\cdot\cos i_1 & -\dfrac{\overline{V}}{\gamma_2}\cdot\alpha_2\cdot g\cdot\cos i_2\end{bmatrix} \tag{C-6b}$$

$$V_1+V_2=\frac{1}{gh}\begin{bmatrix}\delta_1^B\alpha_1\cdot h\cos i_1 & \delta_2^B\alpha_2\cdot g\cos i_2\\ \tilde{U}\cos i_1 & -\tilde{V}\cos i_2\end{bmatrix} \tag{C-6c}$$

$$(V_1+V_2)^{-1}=\frac{gh}{(\tilde{\Delta}+\tilde{\nabla})\cos i_1\cos i_2}\begin{bmatrix}\tilde{V}\cos i_2 & \delta_2^B\alpha_2\cdot g\cos i_2\\ \tilde{U}\cos i_1 & -\delta_1^B\alpha_1\cdot h\cos i_1\end{bmatrix} \tag{C-6d}$$

$$S_{11}=\frac{ap\cdot gh}{\tilde{X}(\tilde{\Delta}+\tilde{\nabla})}\cdot\begin{bmatrix}\dfrac{1}{\beta_1}(\overline{R}\tilde{V}+\rho_2\overline{G}\tilde{U}) & \dfrac{1}{\beta_1}\left(\overline{R}\cdot g\alpha_2\cdot\delta_2^B-\rho_2\overline{G}\cdot h\alpha_1\cdot\delta_1^B\right)\\ -\dfrac{1}{\beta_2}(\rho_1\overline{H}\tilde{V}+\overline{Q}\tilde{U}) & -\dfrac{1}{\beta_2}\left(\rho_1\overline{H}\cdot g\alpha_2\cdot\delta_2^B-\overline{Q}\cdot h\alpha_1\cdot\delta_1^B\right)\end{bmatrix} \tag{C-7a}$$

$$S_{21}=\frac{1}{\tilde{\Delta}+\tilde{\nabla}}\begin{bmatrix}\tilde{V}\cdot h\alpha_1 & gh\cdot\alpha_1\alpha_2\cdot\delta_2^B\\ \tilde{U}\cdot g\alpha_2 & -gh\cdot\alpha_1\alpha_2\cdot\delta_1^B\end{bmatrix} \tag{C-7b}$$

The expressions of relevant parameters involved in analytical expressions of the submatrices in Eqs. C-1~C-7 are shown in Tables C-1 and C-2.

Table C-1
Parameter expressions similar to Aki and Richards (1980) in exact analytical expressions

Parameters	Expressions	Parameters	Expressions
a	$\rho_2(1-2\beta_2^2p^2)-\rho_1(1-2\beta_1^2p^2)$	b	$\rho_2(1-2\beta_2^2p^2)+2\rho_1\beta_1^2p^2$
c	$\rho_1(1-2\beta_1^2p^2)+2\rho_2\beta_2^2p^2$	d	$2(\rho_2\beta_2^2-\rho_1\beta_1^2)$
$\overline{G}$	$a-d\dfrac{\cos i_1}{\alpha_1}\dfrac{\cos j_2}{\beta_2}$	$\overline{G}'$	$a+d\dfrac{\cos i_1}{\alpha_1}\dfrac{\cos j_2}{\beta_2}$
$\overline{H}$	$a-d\dfrac{\cos i_2}{\alpha_2}\dfrac{\cos j_1}{\beta_1}$	$\overline{H}'$	$a+d\dfrac{\cos i_2}{\alpha_2}\dfrac{\cos j_1}{\beta_1}$
$\overline{Q}$	$ac+bd\dfrac{\cos i_1}{\alpha_1}\dfrac{\cos j_1}{\beta_1}$	$\overline{Q}'$	$ac-bd\dfrac{\cos i_1}{\alpha_1}\dfrac{\cos j_1}{\beta_1}$
$\overline{R}$	$ab+cd\dfrac{\cos i_2}{\alpha_2}\dfrac{\cos j_2}{\beta_2}$	$\overline{R}'$	$ab-cd\dfrac{\cos i_2}{\alpha_2}\dfrac{\cos j_2}{\beta_2}$
$\overline{E}$	$b\dfrac{\cos i_1}{\alpha_1}+c\dfrac{\cos i_2}{\alpha_2}$	$\overline{F}$	$b\dfrac{\cos j_1}{\beta_1}+c\dfrac{\cos j_2}{\beta_2}$
$\tilde{X}$	$\dfrac{\rho_1\rho_2\overline{GH}-\overline{QR}}{d}=-a(\overline{EF}+\overline{GH}p^2)$		

Table C-2
Parameter expressions related to pores and pore fluids in exact analytical expressions

Parameters	Expressions	Parameters	Expressions
s	$\dfrac{\overline{\alpha}_1\overline{M}_1}{\alpha_1^2}$	l	$\dfrac{\overline{\alpha}_2\overline{M}_2}{\alpha_2^2}$
g	$\alpha_1-\gamma_1\cos i_1$	h	$\alpha_2-\gamma_2\cos i_2$
$\overline{U}$	$(\overline{\alpha}_1+\delta_1^B)\overline{M}_1-s\cdot\gamma_1^2\approx(\overline{\alpha}_1+\delta_1^B)\overline{M}_1$	$\overline{V}$	$(\overline{\alpha}_2+\delta_2^B)\overline{M}_2-l\gamma_2^2\approx(\overline{\alpha}_2+\delta_2^B)\overline{M}_2$
$\tilde{R}$	$(l\rho_1-sb)\overline{R}$	$\tilde{H}$	$(lc-s\rho_2)\rho_1\overline{H}$
$\tilde{G}$	$(l\rho_1-sb)\rho_2\overline{G}$	$\tilde{Q}$	$(lc-s\rho_2)\overline{Q}$
$\tilde{U}$	$\dfrac{\overline{U}}{\gamma_1}\cdot h\alpha_1-\dfrac{gh}{\tilde{X}}\left(\tilde{R}\dfrac{\cos j_1}{\beta_1}+\tilde{H}\dfrac{\cos j_2}{\beta_2}\right)$	$\tilde{V}$	$\dfrac{\overline{V}}{\gamma_2}\cdot g\alpha_2+\dfrac{gh}{\tilde{X}}\left(\tilde{G}\dfrac{\cos j_1}{\beta_1}+\tilde{Q}\dfrac{\cos j_2}{\beta_2}\right)$
$\tilde{\Delta}$	$\tilde{V}h\alpha_1\delta_1^B$	$\tilde{\nabla}$	$\tilde{U}g\alpha_2\delta_2^B$
$\tilde{M}$	$\tilde{V}\delta_1^B+\dfrac{\overline{U}}{\gamma_1}g\alpha_2\delta_2^B$	$\tilde{N}$	$\left(\tilde{U}-\dfrac{\overline{U}}{\gamma_1}h\alpha_1\right)\delta_1^B$
$\tilde{O}$	$\left(\tilde{V}-\dfrac{\overline{V}}{\gamma_2}g\alpha_2\right)\delta_2^B$	$\tilde{P}$	$\tilde{U}\delta_2^B+\dfrac{\overline{V}}{\gamma_2}h\alpha_1\delta_1^B$
$\tilde{A}$	$\overline{R}\cdot g\alpha_2\cdot\delta_2^B-\rho_2\overline{G}\cdot h\alpha_1\cdot\delta_1^B$	$\tilde{B}$	$\rho_1\overline{H}\cdot g\alpha_2\cdot\delta_2^B-\overline{Q}\cdot h\alpha_1\cdot\delta_1^B$

Appendix D. Weak Elastic Assumption on a Porous Media Interface

For further simplify Eqs. (19)–(27), we use the analytical idea of Aki and Richards (1980) for reference, and change the upper and lower parameters of porous media as follows,

$$angles\begin{cases}i=\dfrac{1}{2}(i_2+i_1), & j=\dfrac{1}{2}(j_2+j_1), & k=\dfrac{1}{2}(k_2+k_1),\\ \Delta i=i_2-i_1, & \Delta j=j_2-j_1, & \Delta k=k_2-k_1,\end{cases} \tag{D-1a}$$

$$velocities\begin{cases}\alpha=\dfrac{1}{2}(\alpha_2+\alpha_1) & \beta=\dfrac{1}{2}(\beta_2+\beta_1) & \gamma=\dfrac{1}{2}(\gamma_2+\gamma_1)\\ \Delta\alpha=\alpha_2-\alpha_1 & \Delta\beta=\beta_2-\beta_1 & \Delta\gamma=\gamma_2-\gamma_1.\end{cases} \tag{D-1b}$$

$$Biot\begin{cases}\overline{\alpha}=\dfrac{1}{2}(\overline{\alpha}_2+\overline{\alpha}_1) & \overline{M}=\dfrac{1}{2}(\overline{M}_2+\overline{M}_1)\\ \Delta\overline{\alpha}=\overline{\alpha}_2-\overline{\alpha}_1 & \Delta\overline{M}=\overline{M}_2-\overline{M}_1\end{cases} \tag{D-1c}$$

$$others\begin{cases}\rho=\dfrac{1}{2}(\rho_2+\rho_1) & \delta^B=\dfrac{1}{2}\left(\delta_2^B+\delta_1^B\right)\\ \Delta\rho=\rho_2-\rho_1 & \Delta\delta^B=\delta_2^B-\delta_1^B.\end{cases} \tag{D-1d}$$

where, α represents the mean of the fast P-wave velocities, and $\Delta\alpha$ denotes the difference of the fast P-wave velocities, and other parameters represent similar meanings.

Under the assumptions of weak elasticity and small angle incidence at the interface of porous media, the values of Δi, Δj, and Δk are minimal, and there are the following approximate relationships,

$$\cos\frac{1}{2}\Delta i\approx 1,\quad \frac{1}{2}\Delta i\approx\sin\frac{1}{2}\Delta i\approx\tan\frac{1}{2}\Delta i, \tag{D-2a}$$

$$\cos\frac{1}{2}\Delta j\approx 1,\quad \frac{1}{2}\Delta j\approx\sin\frac{1}{2}\Delta j\approx\tan\frac{1}{2}\Delta j, \tag{D-2b}$$

$$\cos\frac{1}{2}\Delta k \approx 1,$$
$$\frac{1}{2}\Delta k \approx \sin\frac{1}{2}\Delta k \approx \tan\frac{1}{2}\Delta k, \tag{D-2c}$$

Substituting the transformation relationships (Eq. D-1) and approximate expressions (Eq. D-2) into the ray parameter expression (Eq. (13)), the following approximate relationships can be derived,

$$\tan\frac{1}{2}\Delta i \approx \tan i \cdot \frac{\Delta\alpha}{2\alpha}, \tag{D-3a}$$

$$\tan\frac{1}{2}\Delta j \approx \tan j \cdot \frac{\Delta\beta}{2\beta}, \tag{D-3b}$$

$$\tan\frac{1}{2}\Delta k \approx \tan k \cdot \frac{\Delta\gamma}{2\gamma}, \tag{D-3c}$$

Equation D-3 shows that the sinusoidal function of the difference between incident angles of an elastic wave in upper and lower media is directly proportional to reflection coefficient term of the wave velocity, which is consistent with that derived by Wang (1999) in Eq. (6).

As the exact analytical expressions of scattering coefficients (Eqs. (19)–(27)) involve a series of parameters in Table C-1 and C-2, we need to replace equation D-1, D-2, and D-3 into that in C-1 and C-2, and obtain the first- and second-order approximate expressions of the relevant parameters. Among them, the first-order approximate expressions of p, d, a are,

$$p \approx \frac{\sin i}{\alpha}, \tag{D-4a}$$

$$d \approx 2\rho\beta^2\left(2\frac{\Delta\beta}{\beta} + \frac{\Delta\rho}{\rho}\right), \tag{D-4b}$$

$$a = \Delta\rho - dp^2, \tag{D-4c}$$

Here, the first-order approximate expression of the ray parameter p only has a constant term, and its first-order term is zero, and that of a and d have only first-order terms, and their constant terms are zero.

References

Aki, K., Richards, P.G., 1980. Quantitative Seismology: Theory and Methods-, vols. I-II. W.H. Freeman, San Francisco.

Arora, A., Tomar, S.K., 2007. Elastic waves along a cylindrical borehole in a poroelastic medium saturated by two immiscible fluids. J. Earth Syst. Sci. 116 (3), 225–234. https://doi.org/10.1007/s12040-007-0022-6.

Biot, M.A., 1941. General theory of three-dimensional consolidation. J. Appl. Phys. 12 (2), 155–164. https://doi.org/10.1063/1.1712886.

Biot, M.A., 1957. The elastic coefficients of the theory of consolidation. Journal of Applied Mechanices 24 (2), 594–601.

Biot, M.A., 1962. Mechanics of deformation and acoustic propagation in porous media. J. Appl. Phys. 33 (4), 1482–1498. https://doi.org/10.1063/1.1728759.

Bortfeld, R., 1962. Exact solution of the reflection and refraction of arbitrary spherical compressional waves at liquid-liquid interfaces and at solid-solid interfaces with equal shear velocities and equal densities. Geophys. Prospect. 10, 35–67. https://doi.org/10.1111/j.1365-2478.1962.tb01997.x.

Carcione, J.M., Gei, D., Gurevich, B., Jing, B., 2021. On the normal-incidence reflection coefficient in porous media. Surv. Geophys. 42, 923–942. https://doi.org/10.1007/s10712-021-09646-4.

Chabyshova, E., Goloshubin, G., 2014. Seismic modeling of low-frequency "shadows" beneath gas reservoirs. Geophysics 79 (6), D417–D423. https://doi.org/10.1190/geo2013-0379.1.

Chaisri, S., Krebes, E.S., 2000. Exact and approximate formulas for P-SV reflection and transmission coefficients for a nonwelded contact interface. J. Geophys. Res. Atmos. 105 (B12), 28045–28054. https://doi.org/10.1029/2000jb900296.

Chen, X., He, Z., Zhu, S., Liu, W., Zhong, W., 2012. Seismic low-frequency-based calculation of reservoir fluid mobility and its applications. Appl. Geophys. 9 (3), 326–332. https://doi.org/10.1007/s11770-012-0340-6.

Chen, H., Li, J., Innanen, K., 2020. Nonlinear inversion of seismic amplitude variation with offset for an effective stress parameter. Geophysics 85 (4), 299–311. https://doi.org/10.1190/geo2019-0154.1.

Dai, Z.J., Kuang, Z.B., Zhao, S.X., 2006. Reflection and transmission of elastic waves from the interface of a fluid-saturated porous solid and a double porosity solid. Transport Porous Media 65, 237–264. https://doi.org/10.1007/s11242-005-6084-5.

Denneman, A.I.M., Drijkoningen, G.G., Smeulders, D.M.J., et al., 2002. Reflection and transmission of waves at a fluid/porous-medium interface. Geophysics 67 (1), 282–291. https://doi.org/10.1190/1.1451800.

Deresiewicz, H., 1974. The effect of boundaries on wave propagation in a liquid-filled porous solid: XI. Wave in a plate. Bull. Seismol. Soc. Am. 64 (6), 1901–1907. https://doi.org/10.1785/BSSA0640061901.

Deresiewicz, H., Skalak, R., 1963. On uniqueness in dynamic poroelasticity. Bull. Seismol. Soc. Am. 53 (4), 793–799. https://doi.org/10.1785/BSSA0530040783.

Drew, D.A., Cheng, L., Lahey, R.T., 1979. The analysis of virtual mass effects in two-phase flow. Int. J. Multiphas. Flow 5 (4), 233–242. https://doi.org/10.1016/0301-9322(79)90023-5.

Fatti, J., Smith, G., Vail, P., et al., 1994. Detection of gas in sandstone reservoirs using AVO analysis: a 3-D seismic case history using the Geostack technique. Geophysics 59 (9), 1362–1376. https://doi.org/10.1190/1.1443695.

Gassmann, 1951. Elastic waves through a packing of Spheres. Geophysics 16 (4), 673–685. https://doi.org/10.1190/1.1437718, 1951.

Gholami, A., Aghamiry, H., Abbasi, M., 2018. Constrained nonlinear AVO inversion using Zoeppritz equations. Geophysics 83 (3), 1–41. https://doi.org/10.1190/geo2017-0543.1.

Gray, D., Goodway, B., Chen, T., 1999. Bridging the Gap: Using AVO to Detect Changes in Fundamental Elastic Constants, vol. 1999. SEG Technical Program Expanded Abstracts. https://doi.org/10.1190/1.1821163.

Gurevich, B., Ciz, R., Denneman, A.I.M., 2004. Simple expressions for normal incidence reflection coefficients from an interface between fluid-saturated porous materials. Geophysics 69 (6), 1372–1377. https://doi.org/10.1190/1.1836811.

Huang, H., Chao, W., Fei, G., et al., 2015. Zoeppritz equation-based prestack inversion and its application in fluid identification. Appl. Geophys. 12 (2), 199–211. https://doi.org/10.1007/s11770-015-0483-3.

Kumar, R., Kumar, S., Miglani, A., 2011. Reflection and transmission of plane waves between two different fluid-saturated porous half-spaces. J. Appl. Mech. Tech. Phys. 52 (5), 773–782. https://doi.org/10.1134/s0021894411050129.

Kumar, R., Meglani, A., Garg, S., 2013. Influence of imperfect interface on reflection and transmission coefficients of plane waves between two different fluid saturated porous half spaces. Mater. Phys. Mech. 17, 142–157.

Kumar, M., Kumari, M., Barak, M., 2018. Reflection of plane seismic waves at the surface of double-porosity dual-permeability materials. Petrol. Sci. 15, 521–537. https://doi.org/10.1007/s12182-018-0245-y.

Kumar, M., Barak, M., Kumari, M., 2019. Refection and refraction of plane waves at the boundary of an elastic solid and double-porosity dual-permeability materials. Petrol. Sci. 19, 298–317. https://doi.org/10.1007/s12182-018-0289-z.

Kumari, N., 2014. Reflection and transmission of longitudinal wave at micropolar viscoelastic solid/fluid saturated incompressible porous solid interface. Journal of Solid Mechanics 6 (3), 240–254.

Kumari, M., Virender, Kumar, M., 2021. Wave-induced flow of pore fluid in a cracked porous solid containing penny-shaped inclusions. Petrol. Sci. 18, 1390–1408. https://doi.org/10.1016/j.petsci.2021.09.022.

Kumari, M., Barak, M., Kumar, 2017. Seismic reflection and transmission coefficients of a single layer sandwiched between two dissimilar poroelastic solids. Petrol. Sci. 14, 676–693. https://doi.org/10.1007/s12182-017-0195-9.

Liu, X., Greenhalgh, S., 2014. Reflection and transmission for an incident plane shear wave at an interface separating two dissimilar poroelastic solids. Pure Appl. Geophys. 171, 2111–2127. https://doi.org/10.1007/s00024-014-0844-5.

Liu, X., Chen, J., Zeng, J., et al., 2021. An adaptive joint PP and PS AVA inversion using accurate Jacobian matrix. Geophysics 86 (4), 447–461. https://doi.org/10.1190/geo2019-0785.1.

Lo, W.C., Sposito, G., Majer, E., 2009. Analytical decoupling of poroelasticity equations for acoustic-wave propagation and attenuation in a porous medium containing two immiscible fluids. J. Eng. Math. 64, 219–235. https://doi.org/10.1007/s10665-008-9254-y.

Lovera, O.M., 1987. Boundary conditions for a fluid-saturated porous solid. Geophysics 52 (2), 174–178. https://doi.org/10.1190/1.1442292.

Lu, J., Yang, Z., Wang, Y., et al., 2015. Joint PP and PS AVA seismic inversion using exact Zoeppritz equations. Geophysics 80 (5), R239–R250. https://doi.org/10.1190/geo2014-0490.1.

Lu, C.X., 2010. Inverse matrix of 3 X 3 partitioned matrix. J. Lincang Teachers' College, 20 (2), 121–126. (in Chinese).

Mallick, S., 1993. A simple approximation to the P-wave reflection coefficient and its implication in the inversion of amplitude variation with offset data. Geophysics 58 (4), 544–552. https://doi.org/10.1190/1.1443437.

Mojeddifar, S., Kamali, G., Ranjbar, H., 2015. Porosity prediction from seismic inversion of a similarity attribute based on a pseudo-forward equation (PFE): a case study from the North Sea Basin, Netherlands. Petrol. Sci. 12, 428–442. https://doi.org/10.1007/s12182-015-0043-8.

Muskat, M., Meres, M.W., 1940. Reflection and transmission coefficients for plane waves in elastic media. Geophysics 5 (2), 115–148. https://doi.org/10.1190/1.1441797.

Pan, X., Zhang, G., Zhang, J., Yin, X., 2017. Zoeppritz-based AVO inversion using an improved Markov chain Monte Carlo method. Petrol. Sci. 14, 75–83. https://doi.org/10.1007/s12182-016-0131-4.

Passos, L., Figueiredo, D., Grana, D., et al., 2019. Multimodal Markov chain Monte Carlo method for nonlinear petrophysical seismic inversion. Geophysics 84 (5),

M1–M13. https://doi.org/10.1190/geo2018-0839.1.
Ren, H.T., Goloshubin, G., Hilterman, F.J., 2009. Poroelastic analysis of amplitude-versus-frequency variations. Geophysics 74 (6), N41–N48.
Russell, B.H., Hedlin, K., Hillterman, F., Lines, L.R., 2003. Fluid-property discrimination with AVO: a biot-gassmann perspective. Geophysics 68 (1), 29–39. https://doi.org/10.1190/1.1543192.
Russell, B.H., Gray, D., Hampson, D.P., 2011. Linearized AVO and poroelasticity. Geophysics 76 (3), C19–C29. https://doi.org/10.1190/1.3207863.
Sang, K., Yin, X., Zhang, F., 2021. Machine learning seismic reservoir prediction method based on virtual sample generation. Petrol. Sci. 18, 1662–1674. https://doi.org/10.1016/j.petsci.202.
Santos, L., Tygel, M., 2004. Impedance-type approximations of the P-P elastic reflection coefficient: modeling and AVO inversion. Geophysics 69 (2), 592–598. https://doi.org/10.1190/1.1707079.
Sharma, M.D., 2008. Wave propagation across the boundary between two dissimilar poroelastic solids. J. Sound Vib. 314 (3–5), 657–671. https://doi.org/10.1016/j.jsv.2008.01.023.
Sharma, M.D., Gogna, M.L., 1990. Propagation of elastic waves in a cylindrical bore in a liquid-saturated porous solid. Geophys. J. Int. 103 (1), 47–54. https://doi.org/10.1111/j.1365-246X.1990.tb01751.x.
Shuey, R., 1985. A simplification of the Zoeppritz equations. Geophysics 50 (4), 609–614. https://doi.org/10.1190/1.1441936.
Silin, D.B., Goloshubin, G., 2010. An asymptotic model of seismic reflection from a permeable layer. Transport Porous Media 83 (1), 233–256. https://doi.org/10.1007/s11242-010-9533-8.
Silin, D.B., Korneev, V.A., Goloshubin, G.M., et al., 2004. A Hydrologic View on Biot's Theory of Poroelasticity. Lawrence Berkeley National Laboratory Report LBNL. -54459.
Smit, D., 1961. Some aspects of elastic wave propagation in Fluid-Saturated Porous Solids. Geophysics 26 (2), 169–181. https://doi.org/10.1190/1.1438855.
Smith, G.C., Gidlow, P.M., 1987. Weighted stacking for rock property estimation and detection of gas. Geophys. Prospect. 35, 993–1014. https://doi.org/10.1111/j.1365-2478.1987.tb00856.x.
Tomar, S.K., Arora, A., 2006. Reflection and transmission of elastic waves at an elastic/porous solid saturated by two immiscible fluids. Int. J. Solid Struct. 43 (7–8), 1991–2013. https://doi.org/10.1016/j.ijsolstr.2005.05.056.
Vashisth, A.K., Sharma, M.D., Gogna, M.L., 1991. Reflection and transmission of elastic waves at a loosely bonded interface between an elastic solid and liquid-saturated porous solid. Geophys. J. Int. 105, 601–617. https://doi.org/10.1111/j.1365-246x.1991.tb00799.x.
Wang, Y., 1999. Approximations to the Zoeppritz equations and their use in AVO analysis. Geophysics 64 (6), 1920–1927. https://doi.org/10.1190/1.1444698.
Yang, J., Sato, T., 1998. Influence of viscous coupling on seismic reflection and transmission in saturated porous media. Bulletin of the Seismological of America 88 (5), 1289–1299. https://doi.org/10.1785/BSSA0880051289.
Yeh, C.L., Lo, W.C., Jan, C.D., Yang, C.C., 2010. Reflection and refraction of obliquely incident elastic waves upon the interface between two porous elastic half-spaces saturated by different fluid mixtures. J. Hydrol. 395 (1–2), 91–102. https://doi.org/10.1016/j.jhydrol.2010.10.018.
Yin, X., Zhang, S., 2014. Bayesian inversion for effective pore-fluid bulk modulus based on fluid-matrix decoupled amplitude variation with offset approximation. Geophysics 79 (5), R221–R232. https://doi.org/10.1190/geo2013-0372.1.
Yin, X., Zong, Z., Wu, G., 2013. Improving seismic interpretation: a high-contrast approximation to the reflection coefficient of a plane longitudinal wave. Petrol. Sci. 10 (4), 466–476. https://doi.org/10.1007/s12182-013-0297-y.
Yin, X., Liu, X., Zong, Z., 2015. Pre-stack basis pursuit seismic inversion for brittleness of shale. Petrol. Sci. 12, 618–627. https://doi.org/10.1007/s12182-015-0056-3.
Yuan, S., Yang, S., Wang, T., Qi, J., Wang, S., 2020. Inverse spectral decomposition using an l_p-norm constraint for the detection of close geological anomalies. Petrol. Sci. 17, 1463–1477. https://doi.org/10.1007/s12182-020-00490-6.
Zhao, L.X., Han, D.H., Yao, Q.L., et al., 2015. Seismic reflection dispersion due to wave-induced fluid flow in heterogeneous reservoir rocks. Geophysics 80 (3), D221–D235. https://doi.org/10.1190/geo2014-0307.1.
Zhou, D.Y., Yin, X.Y., Zong, Z.Y., 2019. The characteristics of reflection and transmission coefficients of porous medium saturated with an ideal fluid. Ann. Geophys. 62 (5), 1–9. https://doi.org/10.4401/ag-7815.
Zhou, D.Y., Yin, X.Y., Zong, Z.Y., 2020. Closed-form expressions of plane-wave reflection and transmission coefficients at a planar interface of porous media with a normal incident fast P-wave. Pure Appl. Geophys. 177, 2605–2617. https://doi.org/10.1007/s00024-019-02383-1.
Zoeppritz, K., 1919. On the reflection and penetration of seismic waves through unstable layers. Gottinger Nachrichten 1, 66–84.
Zong, Z., Yin, X., Wu, G., 2015. Geofluid discrimination incorporating poroelasticity and seismic reflection inversion. Surv. Geophys. 36, 659–681. https://doi.org/10.1007/s10712-015-9330-6.
Zong, Z., Feng, Y., Yin, X., Li, K., Zhang, G., 2021. Fluid discrimination incorporating viscoelasticity and frequency dependent amplitude variation with offset inversion. Petrol. Sci. 18, 1047–1058. https://doi.org/10.1016/j.petsci.2020.10.001.